

The effect of lithology on erosional processes and landscape evolution in the Kula badlands

An erosion modelling approach



by Kees Teuling

Supervisors:
Selçuk Aksay
Jeroen Schoorl



October 2018
Chairgroup Soil geography and Landscape
Thesis MSc. Earth and Environment
Soil Geography and Earth Surface Dynamics

The effect of lithology on erosional processes and landscape evolution in the Kula badlands
An erosion modelling approach

Kees Teuling, October 2019
940522-827-010
SGL-80436
MSc-thesis Earth and Environment
Specialisation Soil Geography and Earth Surface Dynamics
Wageningen University

Supervisor(s):
S. Aksay MSc.
Dr. J.M. Schoorl
Examiner(s)
Dr. J.M. Schoorl

Chairgroup Soil Geography and Landscape
Phone: +31 317 482024
office.sgl@wur.nl

Postal address:
Postbus 47
6700 AA, Wageningen
The Netherlands

Visiting address:
Gaia (building number 101)
Droevendaalsesteeg 3
6708 PB, Wageningen
The Netherlands

© All rights reserved. No part of this thesis publication may be reproduced, stored in a retrieval system, or transmitted, in any form or any means, electronic, mechanical, photocopying, recording or otherwise, without the prior written permission of either the author or the Wageningen University Chairgroup of Soil Geography and Landscape. Submitted in partial fulfilment of the requirements for the Master of Science degree in Earth and Environment, specialisation Soil Geography and Earth Surface Dynamics at Wageningen University, Chairgroup Soil Geography and Landscape.

Abstract

The badlands area, a barren and semi-arid area with high erosion rates, contains much information on the stratigraphy of Miocene and Plio-Quaternary sediments and erosion rates as they are well exposed in steep gullies and rivers of the Gediz and Selendi catchments. The initiation and causes of development of these badlands are not yet studied in detail, even though this area contains important information for reconstructing the paleo-landscape. It is also still under debate whether the development of Kula badlands is linked to climate change, poor land use or due to active tectonics.

In the light of previous research, reconstructing and calibrating past landscapes, and estimating erosional rates using stratigraphic data are two main goals of this MSc thesis. The intensive erosional process is suggested to be an important factor for the initiation of the Kula badlands, but both the initiation and the development of these dry topographies is not well understood yet.

To investigate the formation of badlands and associated surface dynamics in the area, numerical landscape modelling is performed. The modelling will be focussed on understanding the influence of the stratigraphy of the badlands area on the erosional processes. Furthermore, an analysis of the stratigraphy and geology is carried out with intensive fieldwork to examine past sedimentary environments and compare these with the modelling results.

Based on the fieldwork, multiple cross-sections and a basic stratigraphy has been made of the Plio-Quaternary sediments in the badlands. These were the basis of multiple modelling scenarios to investigate the effect of lithology on landscape evolution. The landscape evolution model LAPSUS was used to investigate the effect of simplified lithology on erosional processes over scenarios of 5000 time steps in the area.

Lithology influences erosion dynamics in the badland area both spatially and in magnitude. Adding simplified stratification to the LAPSUS model causes high incision rates at boundaries between lithological units. This is due to detachment limited upstream limestone plateaus and basalt plateaus. Adding the possibility of incision into different lithological layers creates a situation in which the model is much better able to redistribute the topography of the badlands. At first, the spatial variation in K-factor distribution causes low incision rates in the main badland area. However, after 500 years, an incision pulse in the main gullies begins on the boundary between lower badlands and middle badlands. This pulse causes high erosion rates and spatially very narrow erosion patterns in the main gullies and migrates upstream into the higher badlands in a time span of 5000 years. The presence of lithology causes steeper slopes and, in this case, lower overall erosion rates. The model's capacity of redistribution of material (erosion and sedimentation) in the landscape is increased. Side gullies are less active and plateaus and ridges in the badlands are mostly unaffected. This combination of results gives an indication of a possible cause for the preservation of these plateaus. The model is better capable of redistributing erosional locations, due to a more dynamic erosional surface. The results of these modelling exercises stress the importance of understanding the stratigraphy of an area for interpreting landscape evolution and erosional processes. This effect should not be easily discarded in general, and in the case of the badland area, should be taken into account as very significant.

Contents

Introduction.....	1
Study Area	3
Geological setting and background	5
Methodology.....	9
Mapping and facies analysis.....	9
Focusses in the field	11
Landscape Evolution Modelling using LAPSUS.....	14
Model scenarios	14
Results	20
Stratigraphy.....	20
Regional erosion and sedimentation	23
Local sedimentation	36
Lithological layer specific erosion and sedimentation	37
Discussion	42
Conclusions.....	46
References.....	47

Introduction

The Gediz and Selendi catchments in western Anatolia consist of important sedimentary archives of Quaternary sediment/water supply changes possibly in response to climate control, platform change and volcanic damming (Maddy et al., 2012, 2017).

These two catchments and their surrounding area have been investigated by several authors with a focus on geology, stratigraphy and sedimentation (Ersoy et al., 2010; Tokçaer et al.. Ersoy et al. (2010) conducted a detailed research about the stratigraphy and its connection with tectonic activity of Western Turkey. They suggested that the area has undergone different phases of both extension and compression related deformation, starting from Pre-Miocene to Plio-Quaternary.

Volcanic activity substantially influenced the regional hydrology and dynamics by damming rivers and creating temporary lakes that disrupted the energy and positioning of streams and rivers (Maddy et al., 2007, 2012; van Gorp et al. 2013; 2016). Using landscape evolution modelling, the influence of volcanic damming on the dynamics of erosion and fluvial responses is also investigated (van Gorp et al., 2014; 2015).

Apart from these researches, the area has been investigated for paleo environment analysis (Veldkamp et al., 2015), the geochronology (Maddy et al., 2008, 2015; Heineke et al., 2016) and archaeology (Kappelman et al., 2008; Lebatard et al., 2014; Maddy et al., 2015). The archaeological findings in the area provide age control figures to support landscape evolution reconstructions.

Additionally, some authors focused on reconstructing the paleo landscapes with a numerical modelling approach using the fluvial archives in the study area and age control with an attempt to understand past erosional processes and rates (van Gorp et al., 2013; 2014; 2015).

The badlands area, a barren and semi-arid area with high erosion rates, contains much information on the stratigraphy of Miocene and Plio-Quaternary sediments and erosion rates as they are well exposed in steep gullies and rivers in the Gediz and Selendi catchments. The initiation and causes of development of these badlands are not yet studied in detail, even though this area contains important information for reconstructing the paleo-landscape. It is also still under debate whether the development of Kula badlands is linked to climate change, poor land use or due to active tectonics.

In the light of previous research, reconstructing and calibrating past landscapes, and estimating erosional rates using stratigraphic data are two main goals of this MSc thesis. The intensive erosional process is suggested to be an important factor for the initiation of the Kula badlands (Westaway et al., 2004), but both the initiation and the development of these dry topographies is not well understood yet.

To investigate the formation of badlands and associated surface dynamics in the area, numerical landscape modelling is performed. The modelling will be focussed on understanding the influence of the stratigraphy of the badlands area on the erosional processes. Furthermore, an analysis of the stratigraphy and geology is carried out with intensive fieldwork to examine past sedimentary environments and compare these with the modelling results. Although van Gorp et al. (2015) have used a similar modelling approach, their

assumption was that the paleo-landscape consisted of one single sedimentary unit. This research aims to document some of the details of stratigraphy and rock structure in the area and apply this information to landscape evolution modelling. Such a high resolution stratigraphy analysis has not been applied in this area before and should provide a unique and detailed view on badlands formation.

Landscape evolution models (LEM) are widely used in geomorphological studies to quantify and explain landscape evolution processes, feedbacks and driving factors (van Gorp et al., 2014). LEM's are mostly driven by a combination of fluvial and hillslope processes and are increasingly effective in modelling long scale erosional processes and landscape evolution (Tucker & Hancock, 2010).

The studies on the effect of lithology on erosional processes have largely been focussed on solid bedrock rock types and larger geological time scales (Gibbs & Kump, 1994). Differences in erosion rates and sediment yields between different rock types are found, as depicted in Figure 1 (Hicks et al., 1996). It is often concluded that the effect of lithology is of importance in geomorphological studies (Riebe et al., 2001), but is not often researched in a sedimentary archives such as the Kula badlands.

Variation of suspended sediment yields around New Zealand

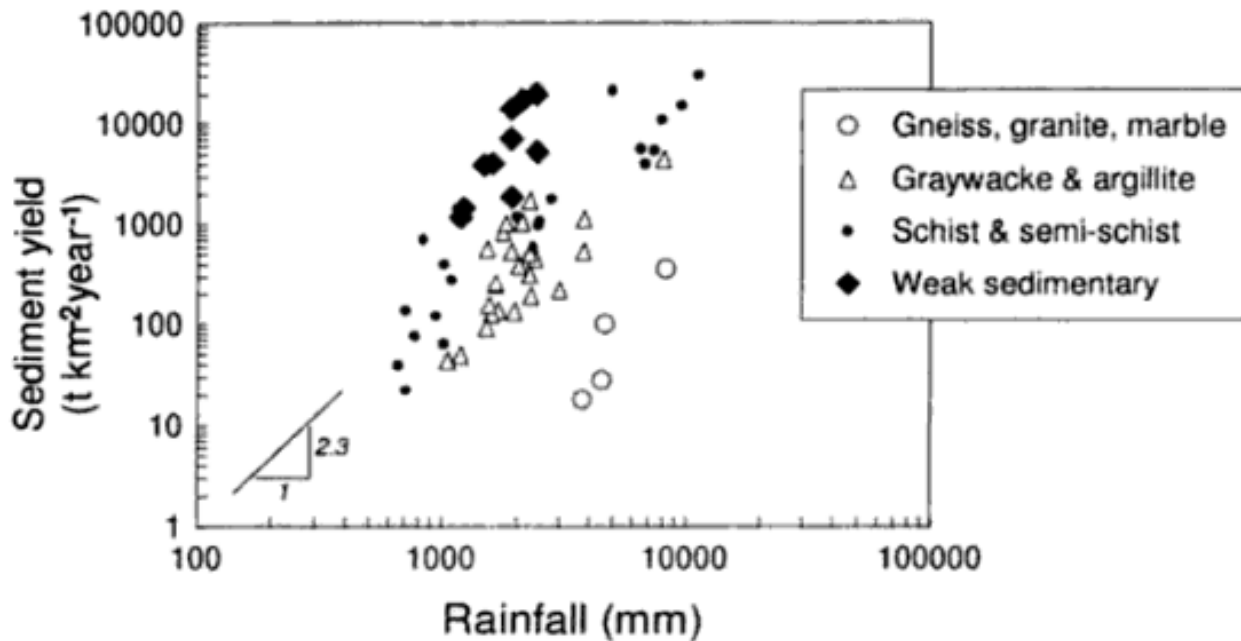


Figure 1 Sediment yield plotted against mean annual rainfall for basins on selected rock types. (Taken from (Hicks et al., 1996))

Study Area

The badlands are located in the headwaters of the Geren, Hudut and Selendi (also known as Kuyu) catchments (Figure 2). The Geren drains into the Gediz river in the south western part of the catchment. The Geren catchment has an area of almost 43km² and an altitude range from 340 to 865 meters (Figure 3). As was mentioned before, the badlands area is characterised by relatively flat slightly tilting plateau remnants, dissected by numerous 10 to 20 metres deep gullies and small streams. In the north, a limestone plateau protrude from the landscape. In the south, plateaus covered by basalt at around 600-650 meters altitude stand out in the area. The badlands contain sparse vegetation in small patches and on the steep gully sides, more dense on north facing slopes than on the south facing slopes.

The plateaus that are sometimes situated in between the gullies are exceptions. These plateaus are relatively flat and have a very gentle slope. On some of these plateaus small villages can be found and agriculture is the main source of income. Some of these plateaus do not seem to be prone to intense erosion for a long time in human history. Remains from ancient civilisations (i.e. pottery pieces) can be found in various locations on these levels. These pottery pieces are not dated or investigated, but they do give an indication of some human influence on the past thousands of years.

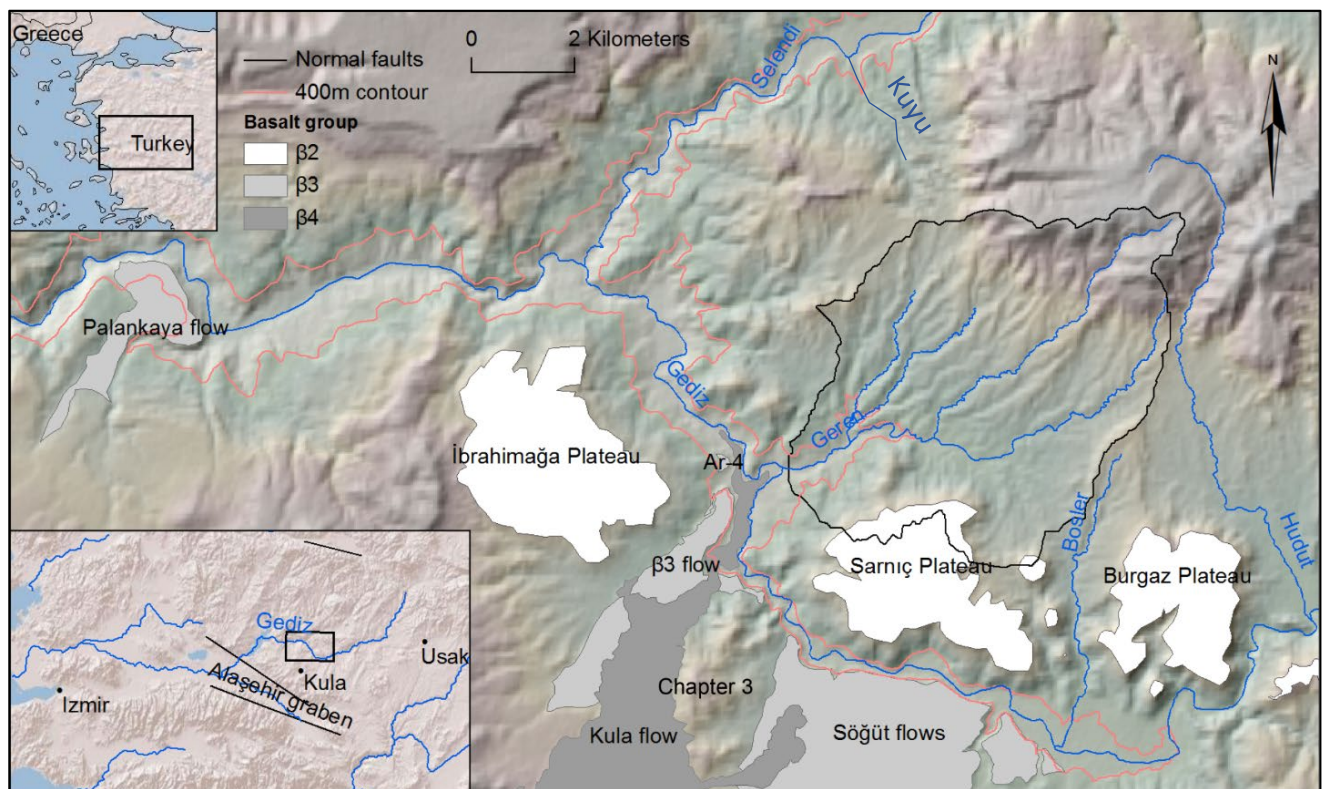


Figure 2 Location of the Geren catchment in western Turkey. (Taken from van Gorp et al., (2013)).

As can be seen in Figure 5, the plateaus in the badlands are relatively flat. At the edges, a steep slope can be seen, in this case with an altitude of around 15 meters, that ultimately reaches the bottom of a gully system. On top of the plateau, agriculture is applied and a village is visible. These lands are property of the people from these villages.

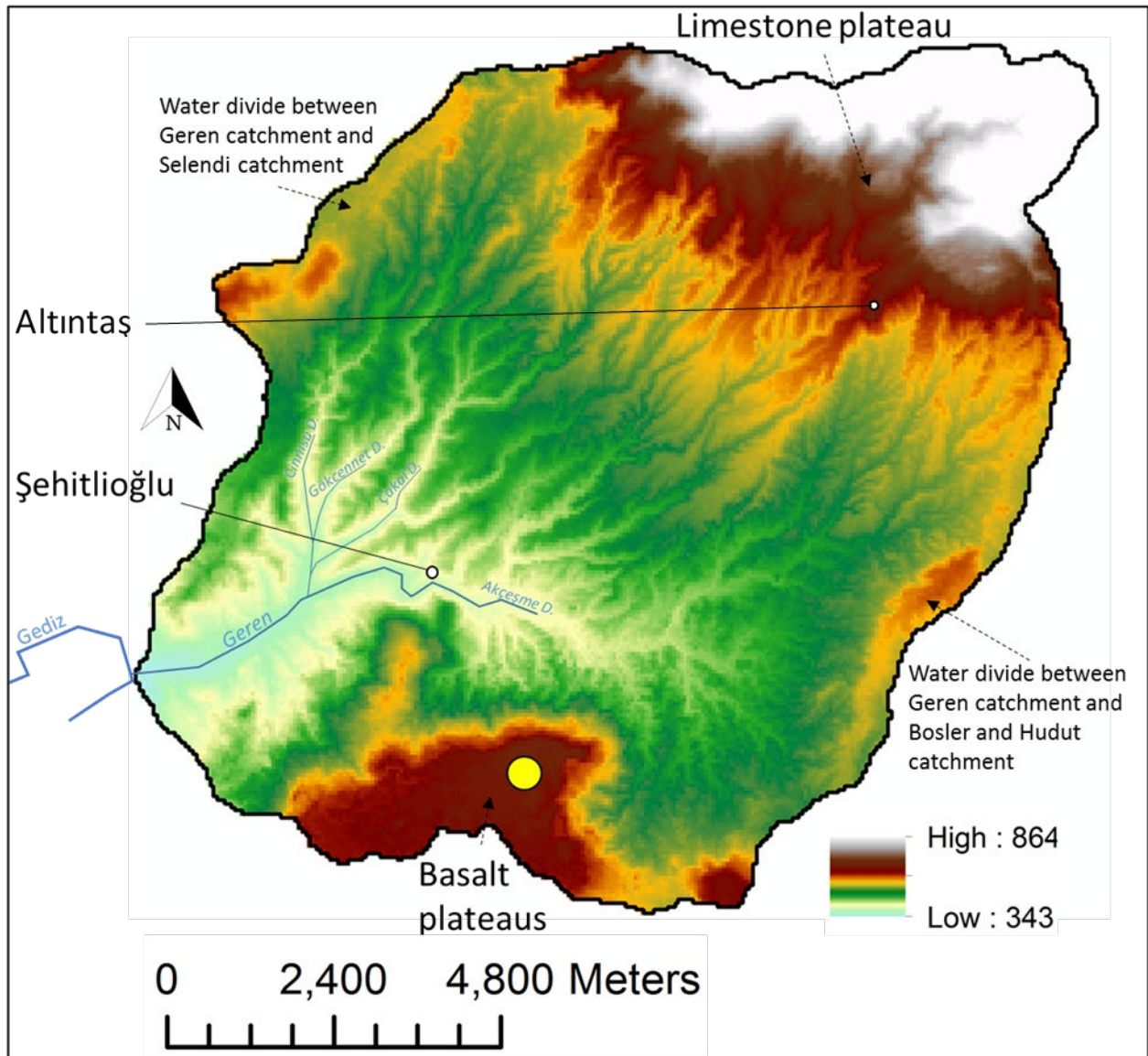


Figure 3 Digital elevation model of the Geren catchment. The yellow circle indicates the position from which Figure 7 is seen.

Geological setting and background

Badlands are generally defined as semi-arid areas with sparse vegetation and high erosion rates which are affected by many driving factors (Bryan & B., 1978; Cantón et al, 2001, 2004;). They occur at many areas in the world, such as Italy (Brandolini et al., 2018), New Jersey, USA (Schumm, 1965), Israel (Yair & Lavee, 1980) and Canada (Campbell, 1989) Badlands have been intensively researched in geomorphological studies for the last thirty years (Gallart et al., 2013).

The Kula badlands are situated on the edge of the Selendi basin, a NE-SW-trending basin. In the north, the smaller Simav graben is situated and in the south the Alaşehir graben is situated (Seyitoğlu & Scott, 1996). After leaving the Selendi basin, the Gediz river flows through this latter graben west-ward until it debouches into the Aegean sea, north of Izmir (Kucuksezgin et al., 2008). The graben systems are mainly SE-NW oriented. Sediments in the badlands are primarily filled with Miocene sedimentary rocks, which lie on top of the metamorphic Menderes Massif, a continental extensional massif (van Hinsbergen, 2010).

According to Ersoy et al. (2010), our study area (i.e. part of Selendi basin according to some authors) has been subject to five phases of deformation. The first phase consisted of strong magmatic activity in the Proterozoic/Cambrian boundary (Gessner et al., 2001). The second deformation phase consisted of detachment faulting in early Miocene. On the following phase, a volcanic activity played a dominant role in the area, which is associated with a NE-SW trending strike slip fault development. This tectonic activity consisted of NE-SW trending sinistral (left-lateral) faults. The fourth deformation refers to late Miocene volcanism, caused by NE-SW trending sinistral faults as well. In the fifth and final deformation contains normal faulting in Plio-Quaternary, in which the Simav and Gediz grabens were likely formed. A visual representation of these events can be seen Figure 4. The final deformation phase caused the Selendi basin to be superimposed with respect to the Simav and Gediz graben.

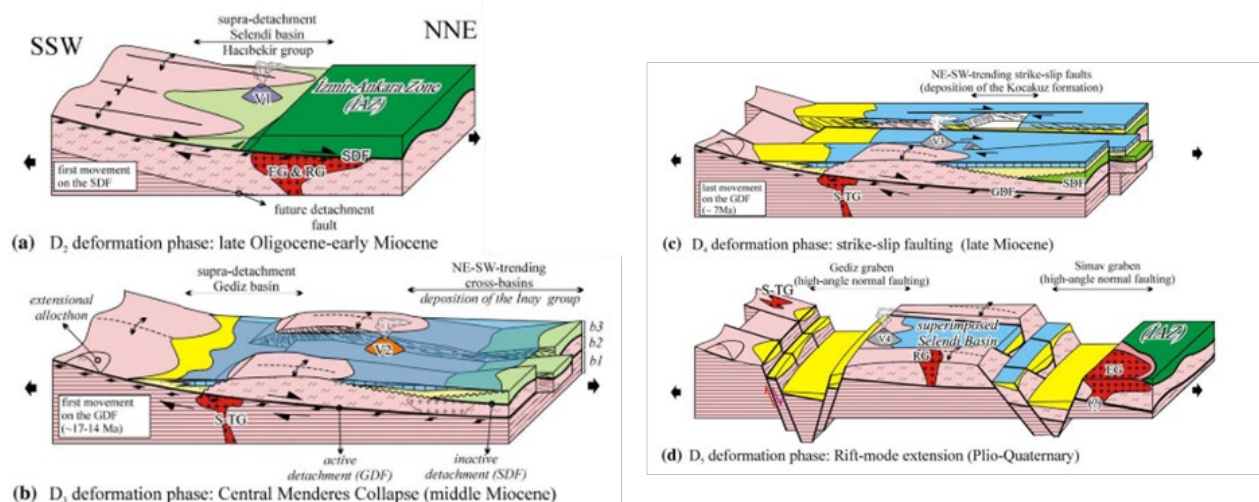


Figure 4 The final four deformation phases according to and taken from Ersoy et al., (2010).

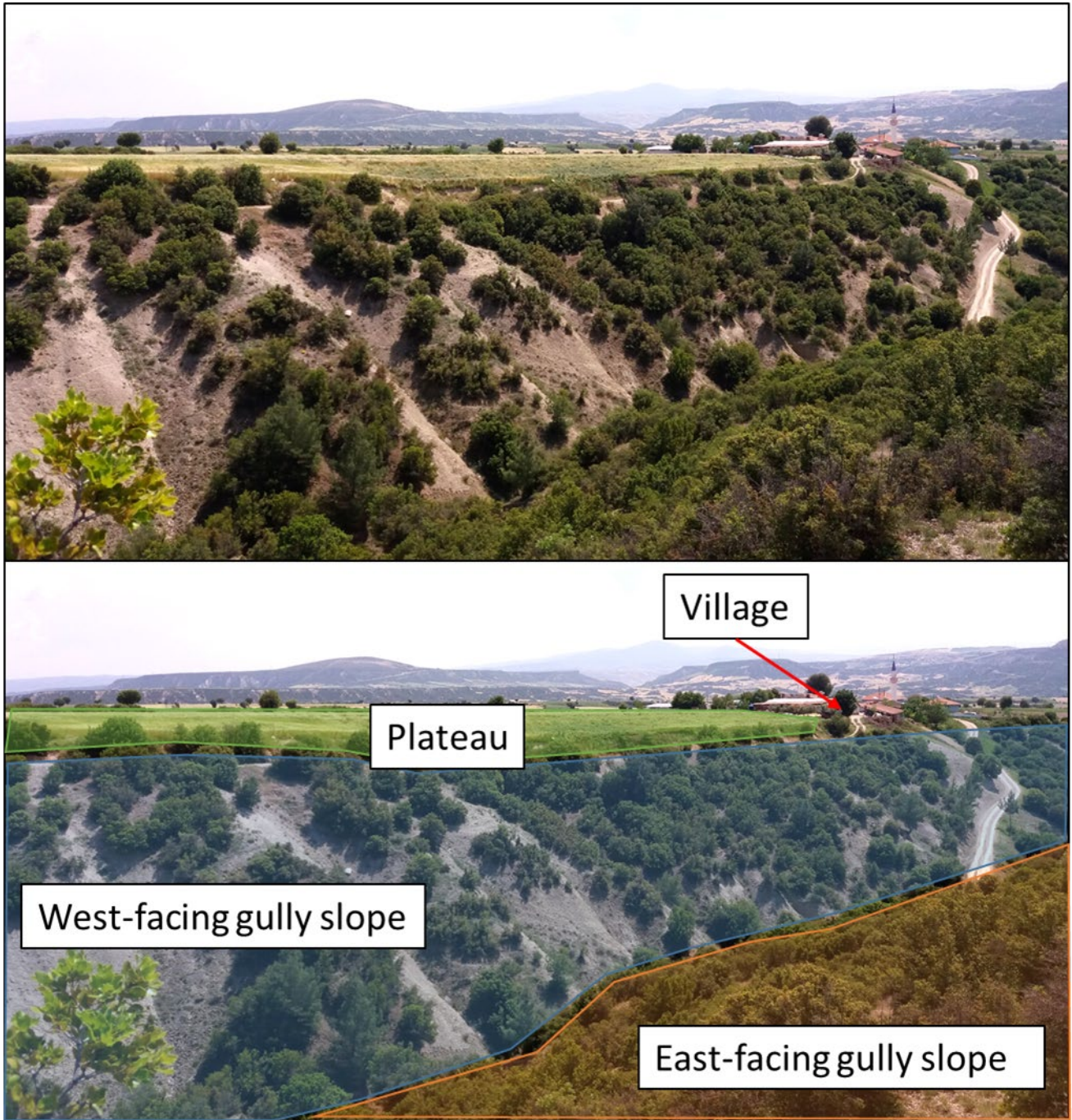


Figure 5 Example of South tilting Plateau in the badland area. Picture is taken southwards. In the distance, the basalt plateaus are visible.



Figure 6 Pottery shards and pieces found throughout the badland area. These pottery pieces are not dated or investigated, but they do give an indication of some human influence on the past thousands of years.

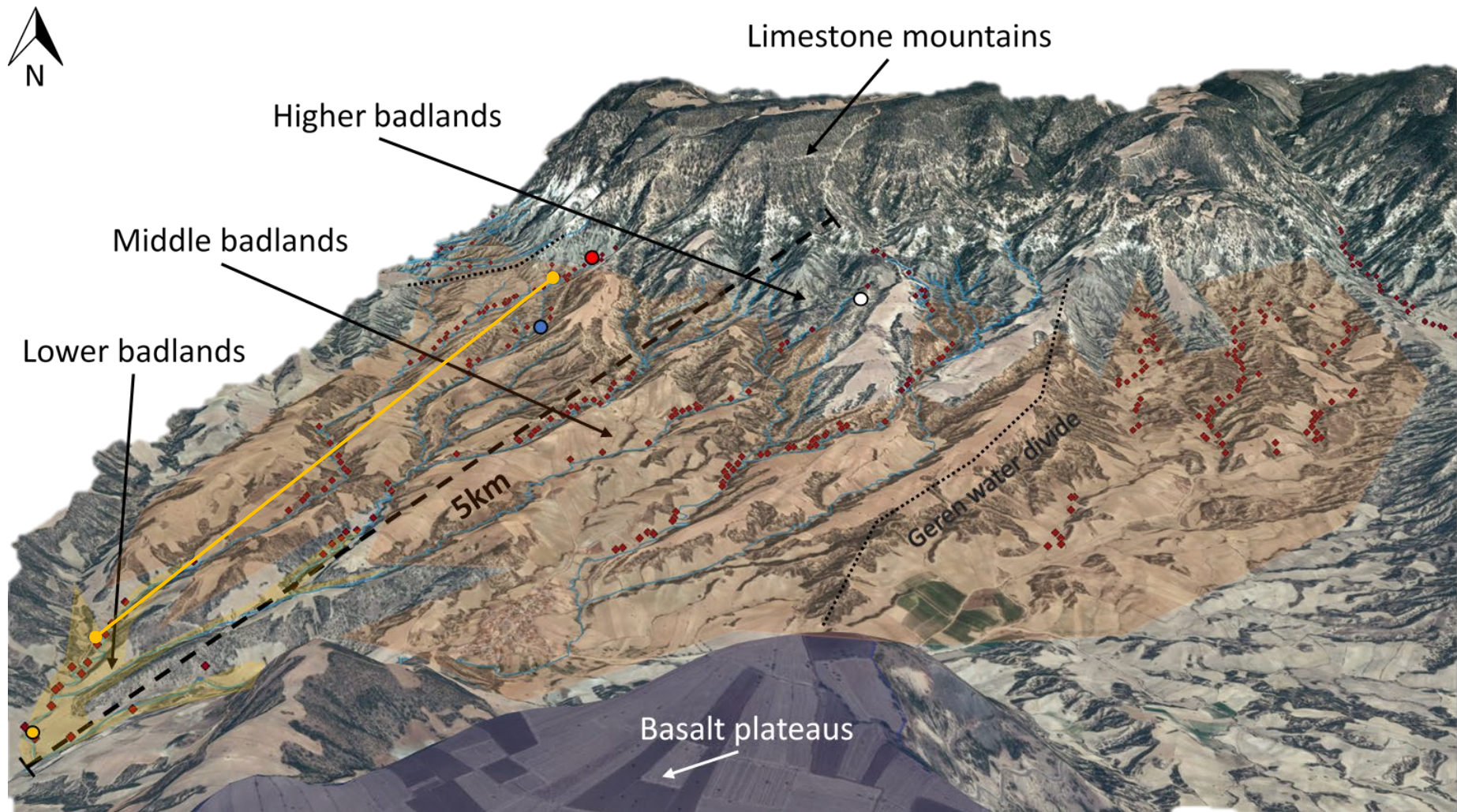


Figure 7 Birds eye view of the Kula badlands area, the subdivision and terminology. The blue lines indicate gullies and the red points are measurement points of the field work. The white circle indicates the position from which Figure 5 was taken. The red and blue circles indicate the position from which Figure 12 was taken. The orange circle indicates the position from which Figure 13 was taken. The yellow line indicates the transect location for Figure 17.

Methodology

Mapping and facies analysis

The fieldwork encompassed a month-long detailed geological mapping and analysis of the stratigraphy and past geological environments in the study area, with a focus on outcrops in a number of rivers and gullies in the badlands area. The goal of examining this stratigraphy was to identify different lithologies and their corresponding depositional environments, as described in Miall (2015). Attempts were made to identify the source of these lithologies as well. Thicknesses and orientation of layers and the rock structure give indications of the geometry, accommodation space and erosion times, and possibly tectonic activity. Further, sorting, grading and imbrication of fluvial sediments were identified in an attempt to understand the energy dynamics and possible flow directions of these environments. These are important for landscape reconstruction, especially in paleo-channels. Local topographic maps and maps from previous work were used for in field support and basic reference. Further field instruments consisted of a compass, geological hammer, hand magnifier, meter and pickaxe. All of these observations will be integrated in a spatial and temporal reconstruction of the paleo-landscape of the Kula badlands. The bulk of data collected in this fieldwork will be used in further research, but it will provide a basis on lithological understanding for the modelling exercises executed in this thesis. A basic representation of the stratigraphy in the so-called Selendi basin can be seen in Figure 8.

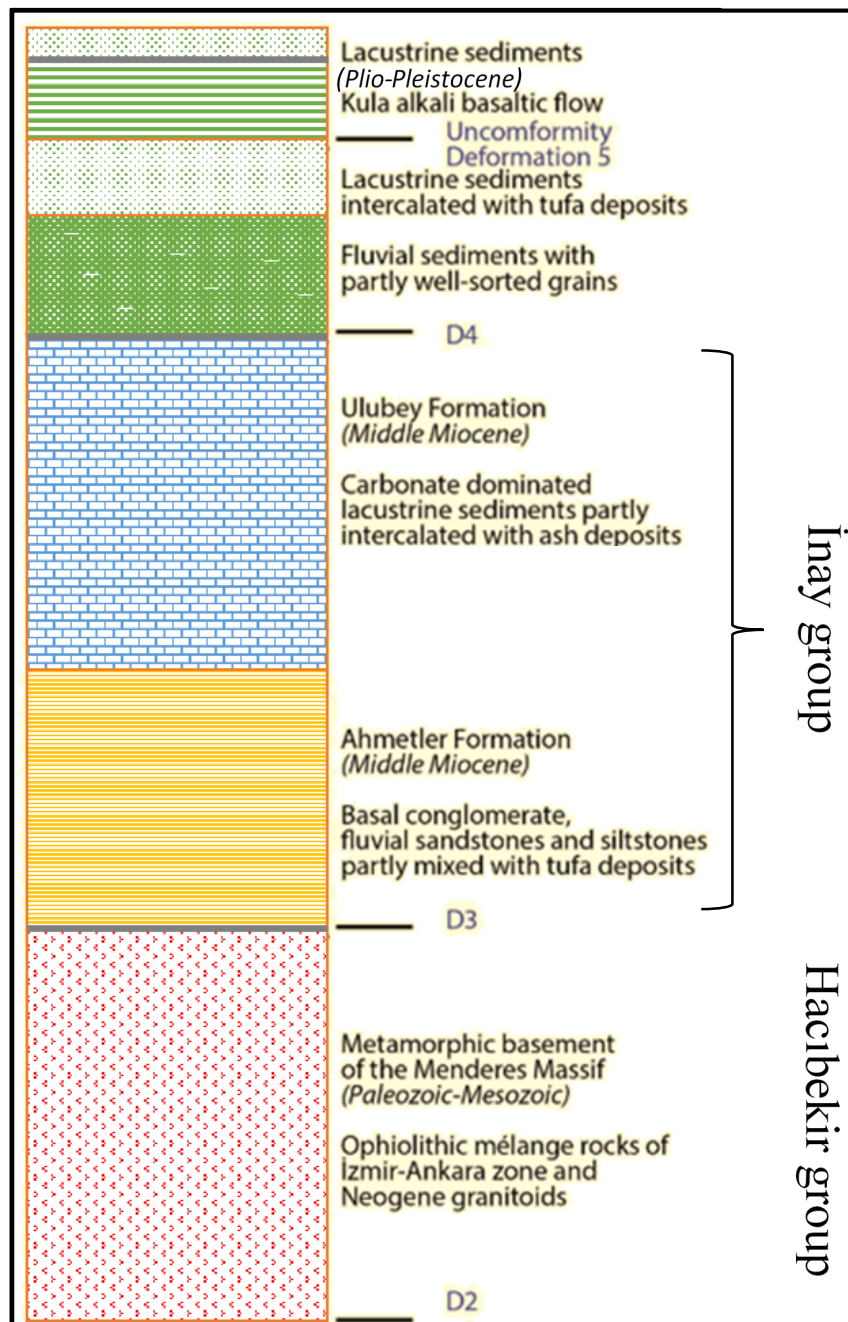


Figure 8 A simplified stratigraphy of the upper layers of the so-called Selendi Basin. (Modified after van Gorp et al., 2013; Maddy et al., 2012; Ersoy et al., 2010.)

Focusses in the field

As mentioned before, the fieldwork focussed on mapping all geological units and documenting the stratigraphy of rock units through gullies and rivers. Data was collected in a transect-like structure roughly N-W extending transects (Figure 7). If clearly preserved, bedding, possible fractures and faults, syn-sedimentary structures and formation unit and boundaries between lithologies and their thicknesses were documented in details with relevant measurements. For every stop, coordinates and altitude are noted as well. These measurements were done using GPS and a compass. Outcrop height and layer thicknesses were measured using measuring tape and a laser-rangefinder.

The bedding and fault planes were measured by placing the compass perpendicular on the strike of the bedding plane. This measurement is the bedding plane angle from the north, namely the azimuth. Later, the side of the compass was placed again perpendicular to the bedding/fault plane strike. This measurement is the dipping angle of the plane (Figure 9). The bedding measurement indicates the direction and angle of the deposit at that location. When the same material can be found elsewhere, and bedding measurements are possible to take, these locations can be interpolated to create a cross section.

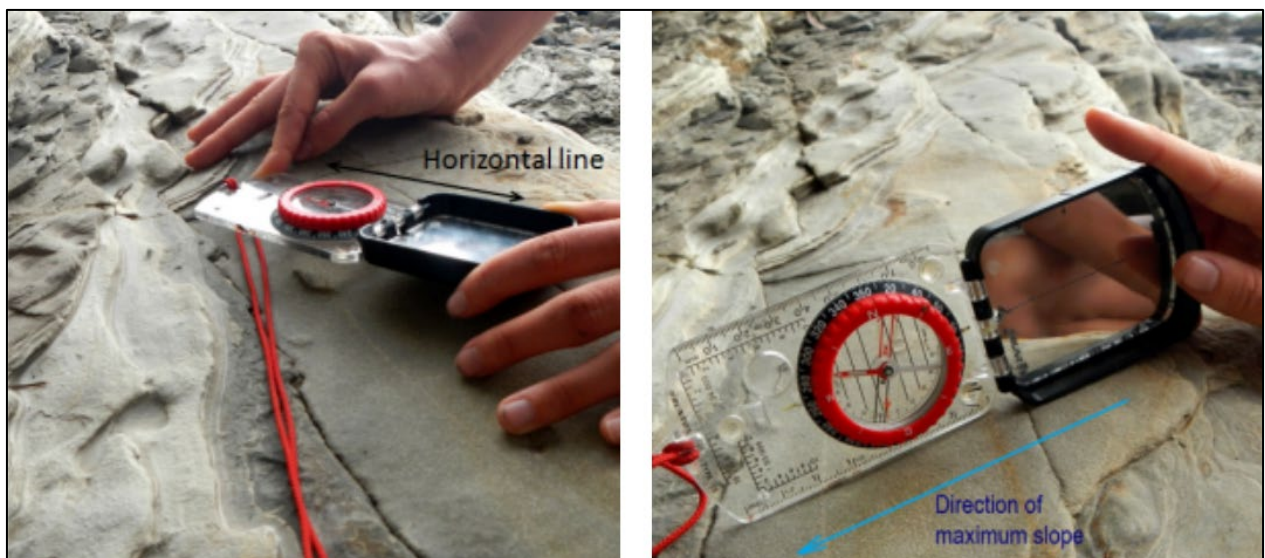


Figure 9 Method of measuring the bedding (left) and the dip angle (right). (Taken from Physical Geology by Steven Earle, chapter 12.4 - figure 12.19)

Sedimentary rocks are often characterized by beddings, which subdivide the depositional environments of a single sedimentary formation. The characteristics of the bedding orientation gives information on environmental energy at the time of deposition or deformation phases after the deposition. Changes in bedding orientation or the stratification in fluvial settings might indicate a change in energy at the time of deposition, which likely happened in the environment as can be seen in Figure 10. The presence of cross-stratification is an indication of the former presence of a fluvial source with a changing depositional energy.

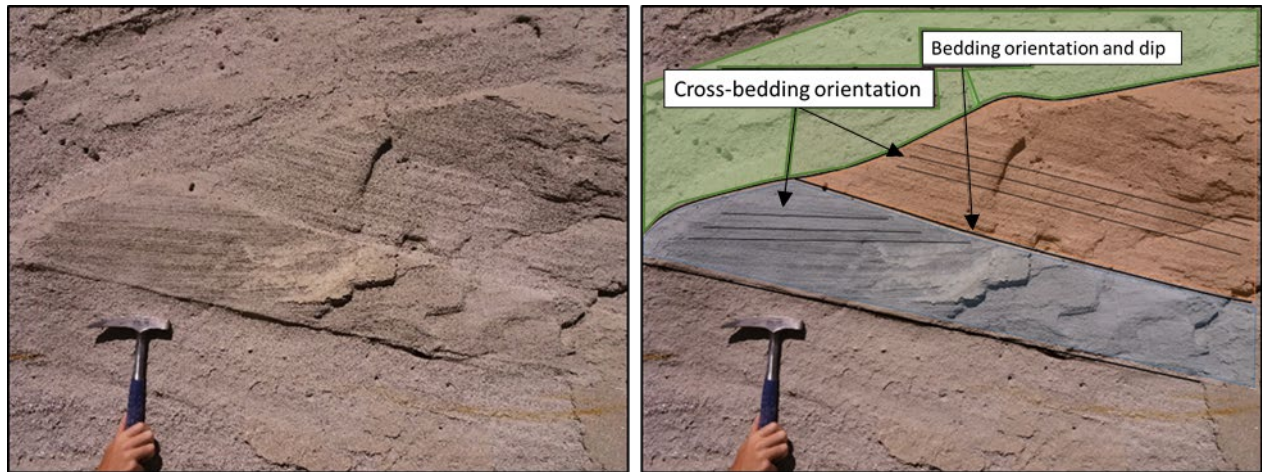


Figure 10 Bedding orientation interpretation. Location is at (6540238,4280333) UTM, picture is taken towards 277°.

Faults in this area are mostly found in Miocene and partly Quaternary sediments. These faults can give information on the tectonic regime for that particular time in the geological history in this area. For example, in Figure 11, a faulting system was documented in Miocene sandstones with displacements of almost 1 meter. The middle part of the structure was pushed up, breaking up the continuity of the layers. In Figure 11, an unconformity between A (Quaternary fluvial sediments) and B (Miocene sandstone) is visible. This means that between the end of the depositional period of B and the beginning of the depositional period of A an erosional period has taken place and it means that the faulting took place before this erosional period. This provides information on accommodation spaces and timings, as well as extra information for the creation of the cross-section. If similar fault systems can be found in other parts of the area, they can be interpolated. This could provide information on larger scale fault systems, which possibly give insights on tectonic regimes and subsequently possible influences on erosional regimes.

After the manual mapping in the field, the field data, like rock units, formation boundaries and measurements of bedding planes, faults and imbrications, were implemented in ArcGIS. Also, the data is manually drawn to visualize the detailed lithologies of separate cross sections based on bedding measurements and faulting. These maps are used to define the boundary conditions and scenarios for the landscape evolution modelling.

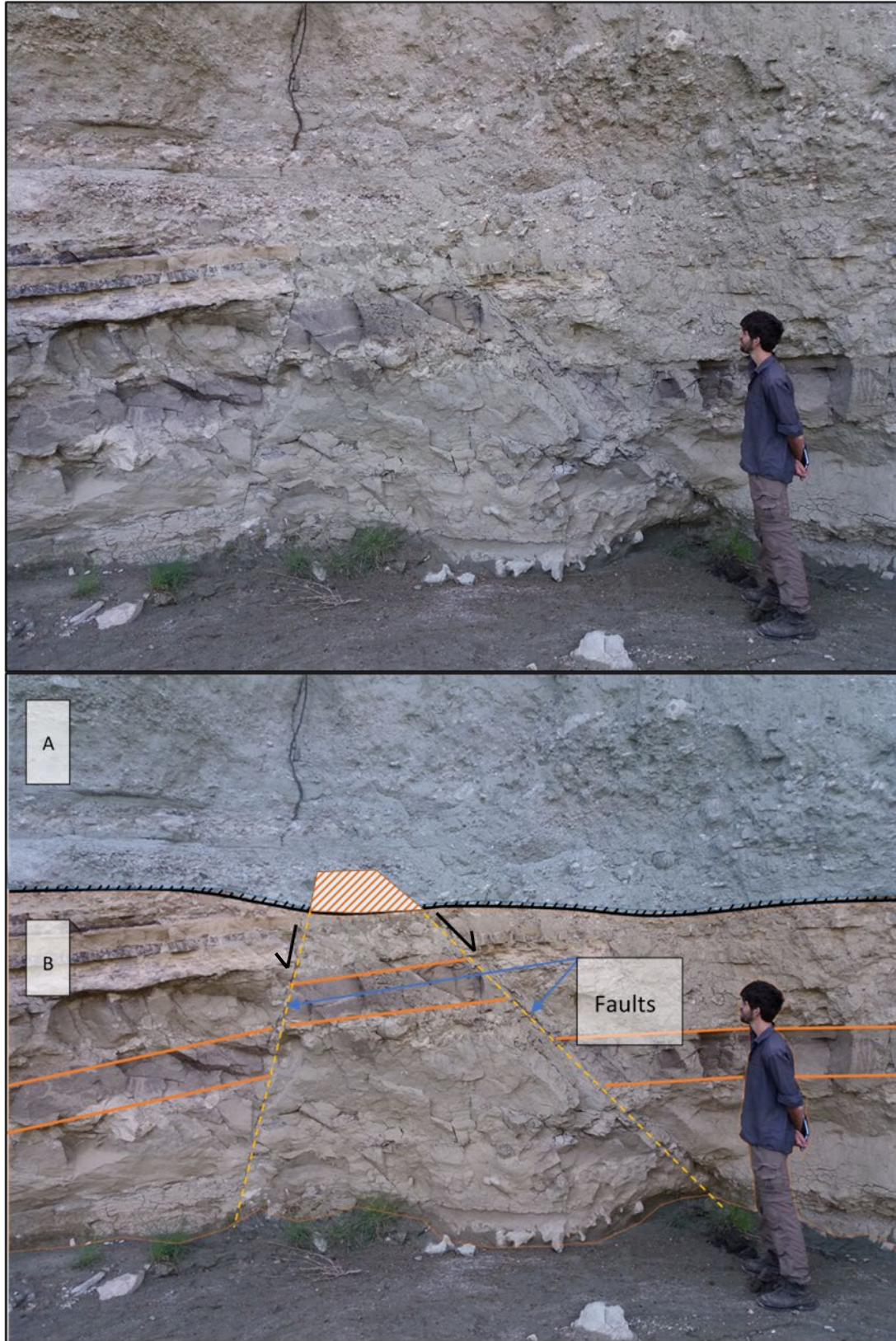


Figure 11 Fault measurement interpretation. Location is at (652190,4285123) UTM, picture is taken towards 272°.

Landscape Evolution Modelling using LAPSUS

For landscape evolution modelling LAPSUS is used. LAPSUS is a reduced-complexity numerical landscape evolution model, that focusses on erosion and sedimentation processes (Schoorl et al., 2000; 2002). The model is able to process landscape configurations and is mostly dependent on gradients and water supply. Dynamics of the area that are found in the field can be implemented in LAPSUS modelling, which makes this model suitable for this research. Reconstruction of paleo topographies using LAPSUS is conducted in Kula badlands also in earlier research (van Gorp et al., 2014; 2015).

LAPSUS requires several basic inputs to function. The geometry of the area is represented by a DEM, the climate is represented by mean annual rainfall and evaporation quantities and the erosional processes are implemented using five parameters: the exponent of overland flow (m), the exponent of slope (n), the multiple flow factor (p), the erodibility (K-factor) and the sedimentability (P-factor). Especially the erodibility is important, as this parameter will be used to calibrate the model for this research area. Tectonics can be implemented as well in the form of both tilting and vertical uplift rates.

A DEM of the Geren catchment is made available by (van Gorp et al., 2015), which has a resolution of 30x30m. It is a DEM created from ALOS-PRISM stereo-satellite imagery and re-scaled to a 30x30m resolution. This DEM is used to model this catchment, incorporating the stratigraphic data of the fieldwork. The LAPSUS model does not have a function to add stratigraphic data, so this is added in the code for the purposes of this research. This gives the opportunity to define different scenarios of the landscape and stratigraphy with different levels of complexity. The results of this simulation and the results of the fieldwork will eventually be integrated to understand the influence of the stratigraphy on the development of badlands in the Kula area. A comparison of scenarios will be investigated to understand the sensitivity of the model and the landscape genesis to the lithology. The scenarios are designed to be in an increasing order of model complexity.

Model scenarios

Four different model scenarios are defined to investigate the effect of lithology on erosion and sedimentation dynamics. To be able to properly analyse this effect, subtle steps of complexity must be taken, regarding the implementation of lithological layers. A lithological layer is defined in the model as a fixed, horizontal layer at a defined altitude in the area. This layer acts as a border between two different lithologies, or, as it is been defined in the model, two different K-factors. The lithology used in the model is a very crude version of the global stratigraphy in the area. Should the actual complex lithology of this area be implemented, the results would be hard to interpret at this stage in the research. This is why in this thesis, the focus will lie on the general effect of lithology on erosional processes.

The first scenario (S1) is the zero scenario. In this scenario, the model does not contain any lithological layers. It contains the configuration of the landscape according to the dynamics calculated by the base model, with one single K-factor value. This scenario acts as a base reference for the effect of lithological layers. The K-factor is based on realistic erosion rates for Mediterranean catchments, this is further explained in the results section. Every scenario has a run time of 5000 years, or 5000 events. The precipitation is 0.555 meters per year (a typical precipitation in a Mediterranean climate) and the

evaporation is set to the factor of 0.35. There will be no implementation of land use, climate change or tectonics or base level change, since that would only add more parameters (i.e. complexity) and more uncertainty.

In the second scenario (S2), two lithological borders are defined. These borders define the boundaries of differences in the K-factor. The area is divided in three K-factor layers, which will stay stable through time. The K-factor is distributed in such a way that the lower badland areas (an altitude of below 400 meters) is appointed a relatively high K-factor and the higher badlands area (above 600 meters altitude) is appointed a relatively low K-factor (Figure 14). The middle badlands area (between 400 and 600 meters altitude) is appointed a value from the first scenario. The extreme K-factors are the factor of 0.5 and 2 of the middle K-factor. As was mentioned before, this distribution of K-factors is based on the global lithology of the study area. The upper area consists of limestone mountains and basalt plateaus, with a relatively low erodibility. The badlands are relatively more easy to erode, hence the somewhat higher K-factor (Figure 12). The lower badlands area consists more of fluvial sediments (Figure 13).

In scenario 3 (S3), the K-factor distribution is similar to scenario 2. However, if a lithological layer is incised in time, the cell in which this happens will inherit the underlying K-factor as well.

In scenario 4 (S4) a third lithological boundary is added. The middle area is separated into two areas. The lower area (between 400 and 500 meters altitude) is assigned the relatively low K-factor and the higher area (between 500 and 600 meters altitude) is assigned the same K-factor as the value used in the first scenario. This is based on the lithological research, in which two different sandstones were found. The bottom sandstone layer is thought to be Miocene sandstone with a lower erodibility and the upper sandstone layer is thought to be of Pliocene age. This sandstone is less compact and easier to erode (Figure 12).



Figure 12 Impression of the upper badlands (above picture), taken at (653884,4283264) UTM and towards 30°. Pliocene sandstones with muddy/silty layers, highly erodible material. And an impression of the middle badlands (lower picture), taken at (653601,428229) UTM and towards 250°. Miocene sandstone, more compacted material, less prone to erosion.



Figure 13 Impression of the lower badlands, taken at (651320,4279252) UTM and towards 255°. Fluvial layers (blue layer), relatively loose material and large grain size. Relatively easy to erode.

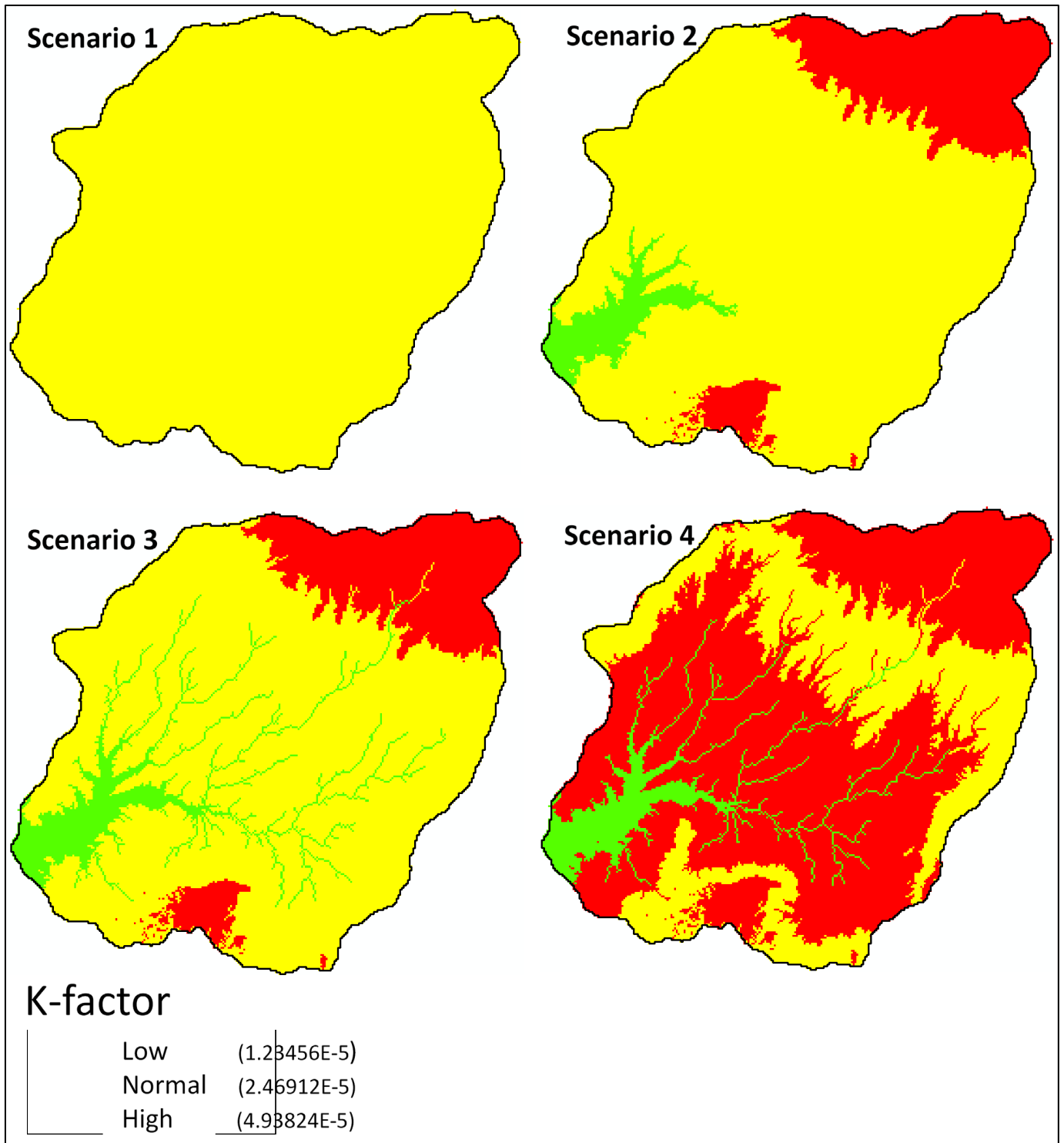


Figure 14 K-factor value distribution in the four defined scenarios.

Figure 15 shows a topographic profile of the Geren catchment from south to north. In this profile the lithological layers as defined in the model scenarios are represented by the four coloured layers. To be able to better analyse the differences in erosion and sedimentation dynamics between scenarios, the total erosion and sedimentation are calculated for every layer. Layer 1 represents the limestone mountains and basalt plateaus (600 meters and higher), layer 2 represents the upper badlands (between 500 and 600 meters), layer 3 the middle badlands (between 400 and 500 meters) and layer 4 the lower badlands (lower than 400 meters).

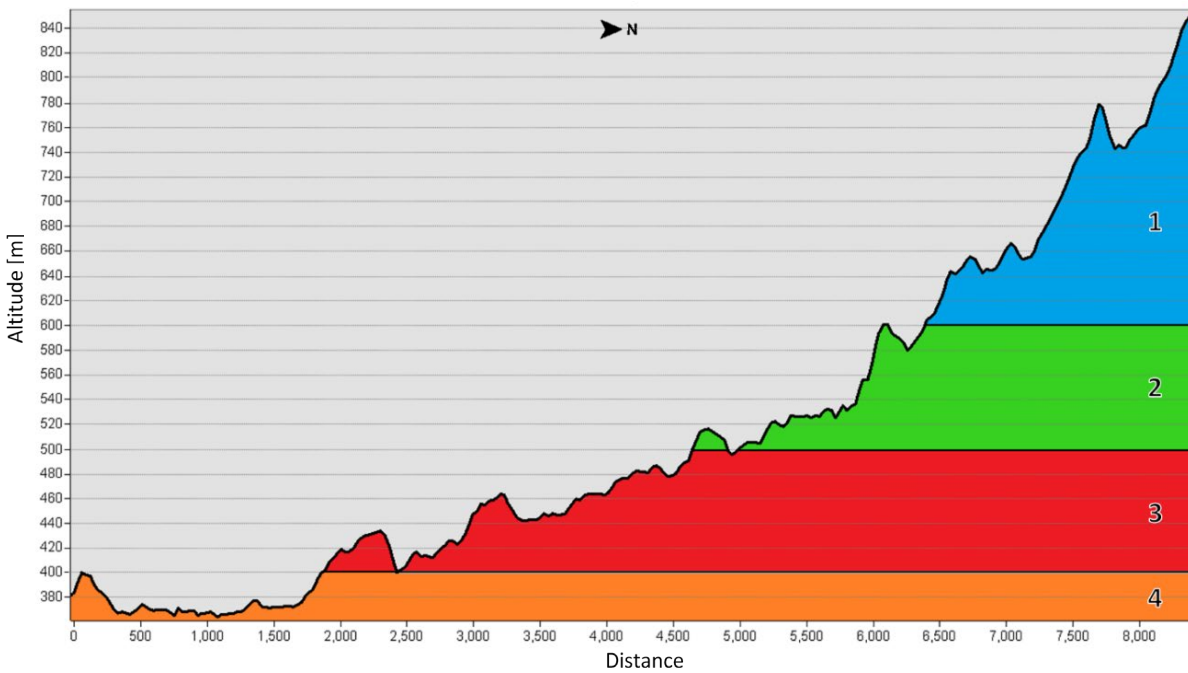


Figure 15 Topographic profile including the layering of the model scenarios.

Results

Stratigraphy

During the fieldwork, facies analysis is conducted to produce a detailed stratigraphy of the area. A basic stratigraphy is created based on cross-sections. This interpretation of the stratigraphy can be seen in Figure 16.

System	Series	Stage	Lithology	Thickness	Further description
Quaternary	Holocene	Late	Poorly sorted fluvial deposits with basalt, limestone, pottery, metamorphic material	30	Cyclic depositional energy changes expressed in differences in grain size.
		Middle	Poorly sorted fluvial deposits with basalt, limestone and metamorphic material	0	From fine grained silty sand to small pebbles. Sometimes directly on top of Miocene sandstone. Cross laminations sometimes visible.
		Early	Poorly sorted fluvial deposits with metamorphic and limestone material	-25	Moderately high energy stream or river system. Not found everywhere.
Neogene	Miocene	Middle	Consolidated sandstone (Ahmetler)	-30	Larger grainsize, smaller silt fraction. Unconformity between sandstone and fluvials. Sometimes faults are found.
			Conglomerates	-55	Small pebbles to large rocks, poorly sorted. Well cemented material.
				-58	

Figure 16 Chrono-stratification interpretation of the badland area.

In this research, cross-sections were created to illustrate the basis for the modelling scenarios and to understand the time and place relationship of different lithological units. Figure 17 shows one of these cross-sections. The sandy/muddy fluvials/colluvials (red, E) on top of the profile are defined as typical badland materials. Typical chimney-like badland erosional features are usually formed in places where this material is present. This is what is named as the upper badlands in the model scenarios in this work. In these sediments, layering of certain grain size and colour repeatedly occur, indicating cyclic depositional energy changes. Beneath these sediments, there are partly muddy and silty sandstones yellow in colour (D). These sandstones are defined as the upper part of the middle badlands. Beneath these sandstones, sometimes fluvial deposits can be found (blue, C). These often poorly sorted materials are not found everywhere in the transects and indicate a depositional environment that was similar to a fairly high energy stream or river system based on the grain size and sorting. In these materials, sometimes paleo flow directions could be found. The fluvial deposits, if present, were always found on top of incised sandstone (orange, B). This sandstone (Ahmetler) is more compact than the younger muddy/silty sandstone found above and consists of a smaller silt fraction. The grainsize is generally larger and the colour of the deposits is somewhat darker. These materials are defined as the lower part of middle badlands. In the south-western part of the Geren catchment, conglomerates can be found (purple, A). Poorly sorted material with a very large grainsize. These materials are preserved in the lower badlands. The conglomerates indicate the former presence of a relatively high energy river system (around 2,5

meters thick). It can be seen that there are faint synclines and anticlines in the cross-section. These indicate the former presence of compressional tectonics in the area. The basin is first filled with a thick layer of sandy materials, after which an erosional phase started. The sandstone was incised, after which a depositional phase started in which stream or river systems filled part of the incised sandstones. Energy levels decreased to the point that only sandy, silty and muddy materials were deposited on top of the incised sandstone or fluvial deposits. On top, the badland colluvials are deposited with cyclic energy changes. Interchanging sandy materials with pebbles and muddy materials. In the north east however, the higher situated limestone material is part of the Ulubey formation (Middle Miocene), which is older than the Quaternary deposits. This means that this material is all eroded in the badland areas. Quaternary sediments found in the field often contained limestone material. If not for the simplified nature of this modelling exercise, four different units of Quaternary sediments would have been defined in the stratigraphy based on field findings. These divisions between units are based on what material the deposits consisted of. The differences in composition were based on both the presence and combination of limestone material, basalt, metamorphic rocks and archaeological findings. For this thesis' purposes however, only two Pleistocene and one Holocene unit is defined. Ongoing research, also with the help of luminescence dating and thin sections, will elaborate on this part of the stratigraphy (Aksay, personal communication).

The orientation and thicknesses of different stratigraphic units in Figure 17 are based on bedding measurements using a Brunton geological compass and thickness measurements with the laser-range finder. Based on these measurements, a cross section is made available (Figure 17), revealing continuous layers. As indicated on the cross section, some of these continuous layers are already eroded. The ages are based on previous research (Seyitoğlu, 1997; Ersoy et al., 2010) and the law of superposition.

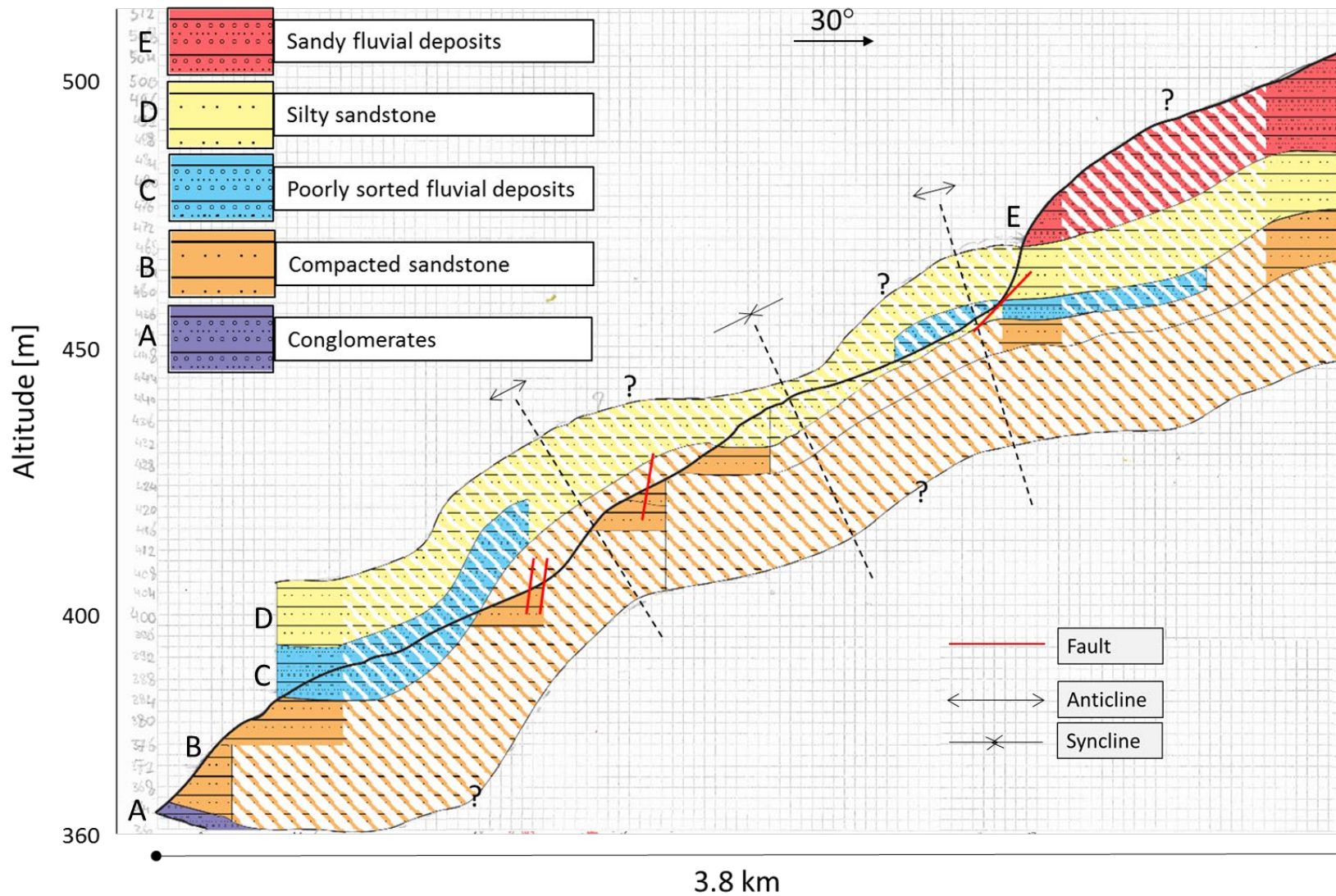


Figure 17 Cross-section of a transect through the badlands area. Fully coloured areas are certainties, dashed areas are interpretations. The thick black line is the actual landscape (gully surface). Everything above is non-eroded materials on the sides of the gullies. Red lines are measured faults. The transect location can be seen in Figure 7. The scale exaggeration between the x-axis and the y-axis is 1:25.

Regional erosion and sedimentation

To investigate the effect of lithology in the dynamics of this area, both temporal and spatial processes in erosion and sedimentation processes are also presented in this work. Through the four defined scenarios, changes in dynamics are monitored and explained.

First, the DEMs are examined. For every scenario in every year, a new DEM is created with the new configuration of altitudes and slopes. Comparing DEMs of different scenarios provides insights in how the erosion and sedimentation dynamics might have changed with the scenario settings.

Figure 18 shows the difference between the DEM of year 5000 and the DEM of year 0 (the original DEM) of all scenarios. The original DEM is subtracted from the 5000 year DEM, creating an image displaying the difference in altitude. Negative values in these maps mean that in total, material has been removed in these 5000 years, but it does not necessarily mean that there has been no sedimentation at these location as well. Positive values indicate more sedimentation than erosion after 5000 years.

As can be seen in Figure 18, in every scenario many tons of hectares of material are eroded in 5000 years, mainly in the gully systems. Outside these gully systems, the area seems more stable with much less material removed. In all four scenarios, only a small amount of areas indicate net sedimentation; the southern part, on the basalt plateaus and small patches in the north-east and the north-west of the area. The general spatial patterns however, seem to remain the same throughout the scenarios.

The highest erosion values can be around 200 meters of removed material in scenario 1 and 250 meters of removed material in scenario 3. Although these values seem large, they are acceptable over a period of 5000 years. It indicates erosion rates of 4 to 5 cm/year in the most extreme locations. (Martínez-Casasnovas, 2003) found gully incision rates of 80 cm/year in north-western Spain for example. The average erosion rate in the badlands is 0.9 mm/year. Cyr & Granger (2008) found average (paleo)erosion rates of 0.20 to 0.58 mm/year in the Apennine mountains in Italy.

There are some differences between the scenarios visible. In scenario 1, high total erosion can be seen in the upper part in the limestone mountains, whereas the magnitude of erosion in this area is limited in the other three scenarios. Furthermore, erosion in the lower part in the south-west is lower in scenario 1 in comparison with the other three. Gully erosion in scenario 4 is less intense in comparison with the other three scenarios.

To be able to better see these differences between scenarios, the total erosion through time in every scenario is plotted in Figure 19 and the differences between scenarios are calculated.

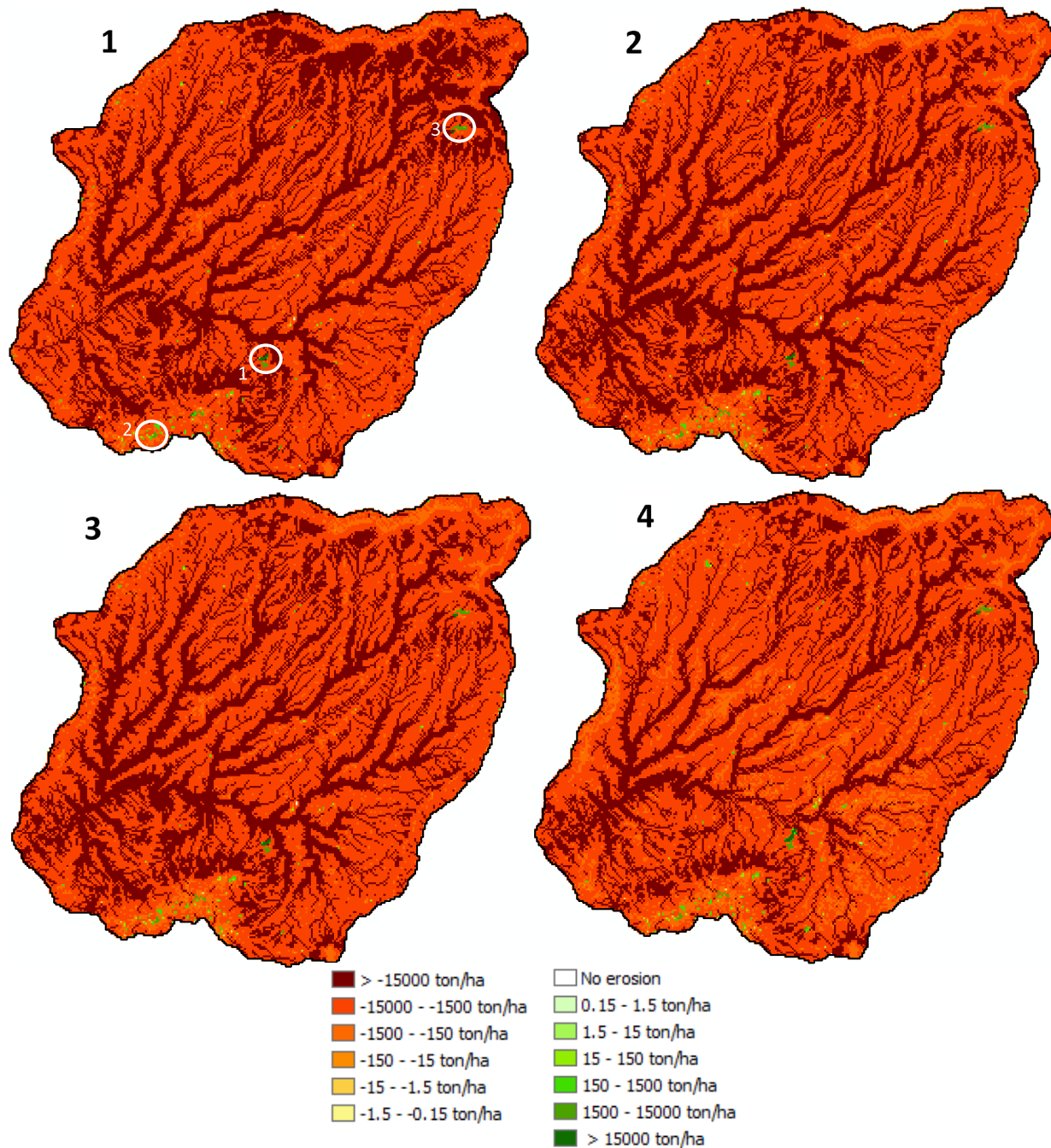


Figure 18 The difference between the 5000 year DEM and the original DEM for all for scenarios. The white circles in scenario 1 indicate deposition areas.

Figure 19 depicts the total erosion for every scenario through time in tons/ha. The erosion in scenario 1 (blue) shows some variations in the first 800 years, after which it becomes relatively constant with a very small and stable decrease in total erosion through time. The average total erosion in scenario 1 over 5000 years is 12.19 tons/ha/year. Scenario 2 (green) starts with a much higher erosion rate of 16 tons/ha/year and then rapidly decreases to 13 tons/ha/year in roughly 400 years. The erosion then decreases with a

relatively constant rate which is slightly higher than the decrease of scenario 1. After 5000 years the average total erosion of scenario 2 is 11.93 tons/ha/year. Scenario 3 (red) starts at around the same erosion rate as scenario 2, but does not share the steep drop in erosion in the first years. Instead it decreases at a relatively stable rate. The small-scale variation is relatively large, creating a spiking time series. After roughly 3500 years, the total erosion hardly seems to decrease. After 5000 years the average total erosion of scenario 3 is 14.01 tons/ha/year. The erosion in scenario 4 (orange) starts at just above 13 tons/ha and decreases at a similar rate as scenario 3. The small-scale variation is larger still than the variation in scenario 3. After 5000 years the average total erosion of scenario 4 is 10.04 tons/ha/year.

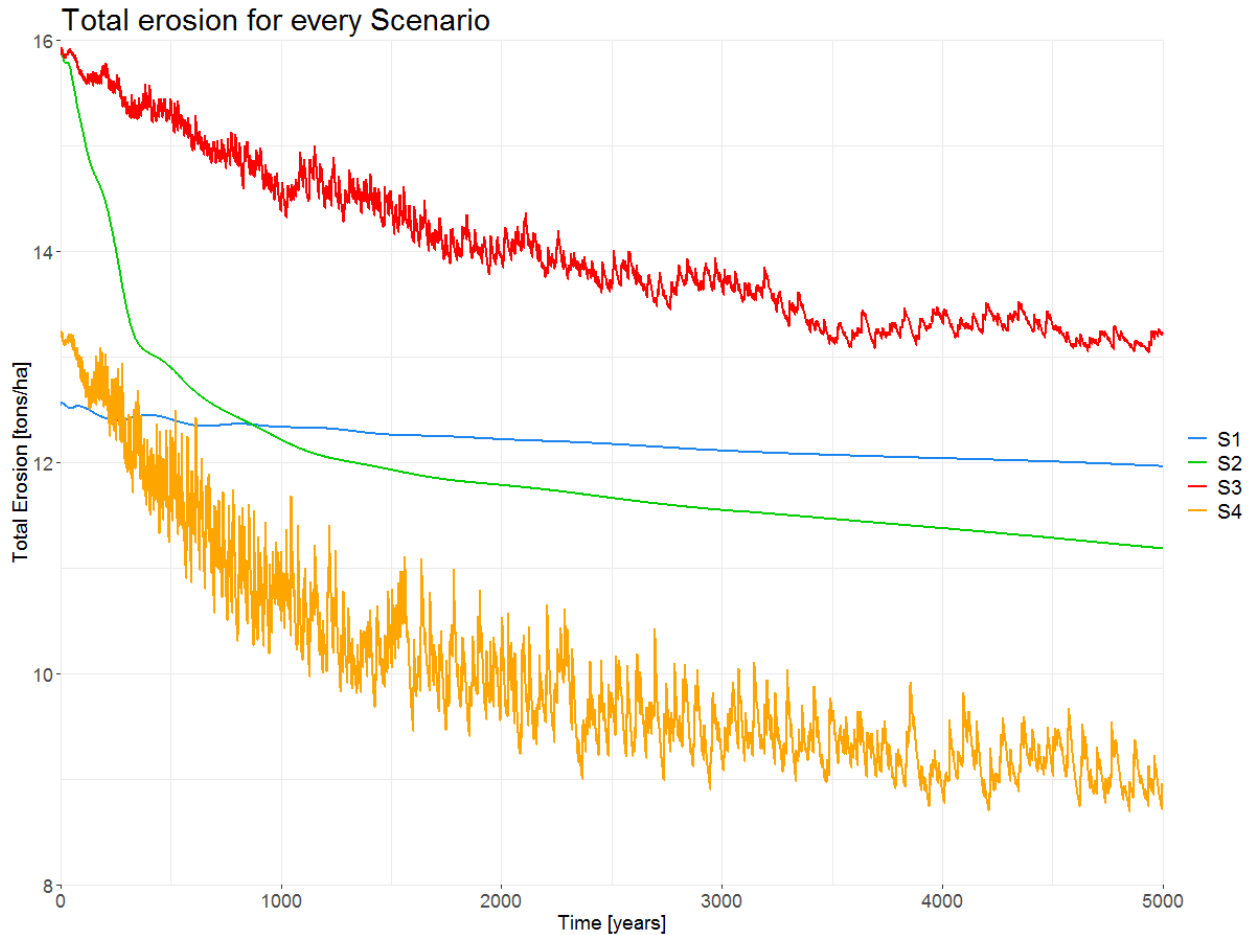


Figure 19 Total erosion for every Scenario. Unit is [tons/ha].

In the first 20 years, the total sedimentation for every scenario is relatively high in comparison with the years after. That is why this graph is split up in two graphs; one representing the total sedimentation in the first 20 years (Figure 20) and one representing year 20 until year 5000 (Figure 21).

The total sedimentation starts relatively high and then decreases sharply for every scenario. The amount of sedimentation is highest in scenario 1 with 0.097 tons/ha and lowest in scenario 4 with 0.066. The sedimentation in scenario 2 and 3 is almost similar in the first year of the configurations with 0.090

tons/ha. Apart from differences in magnitude, the pattern of the diminishing of sedimentation is similar for every scenario (Figure 20).

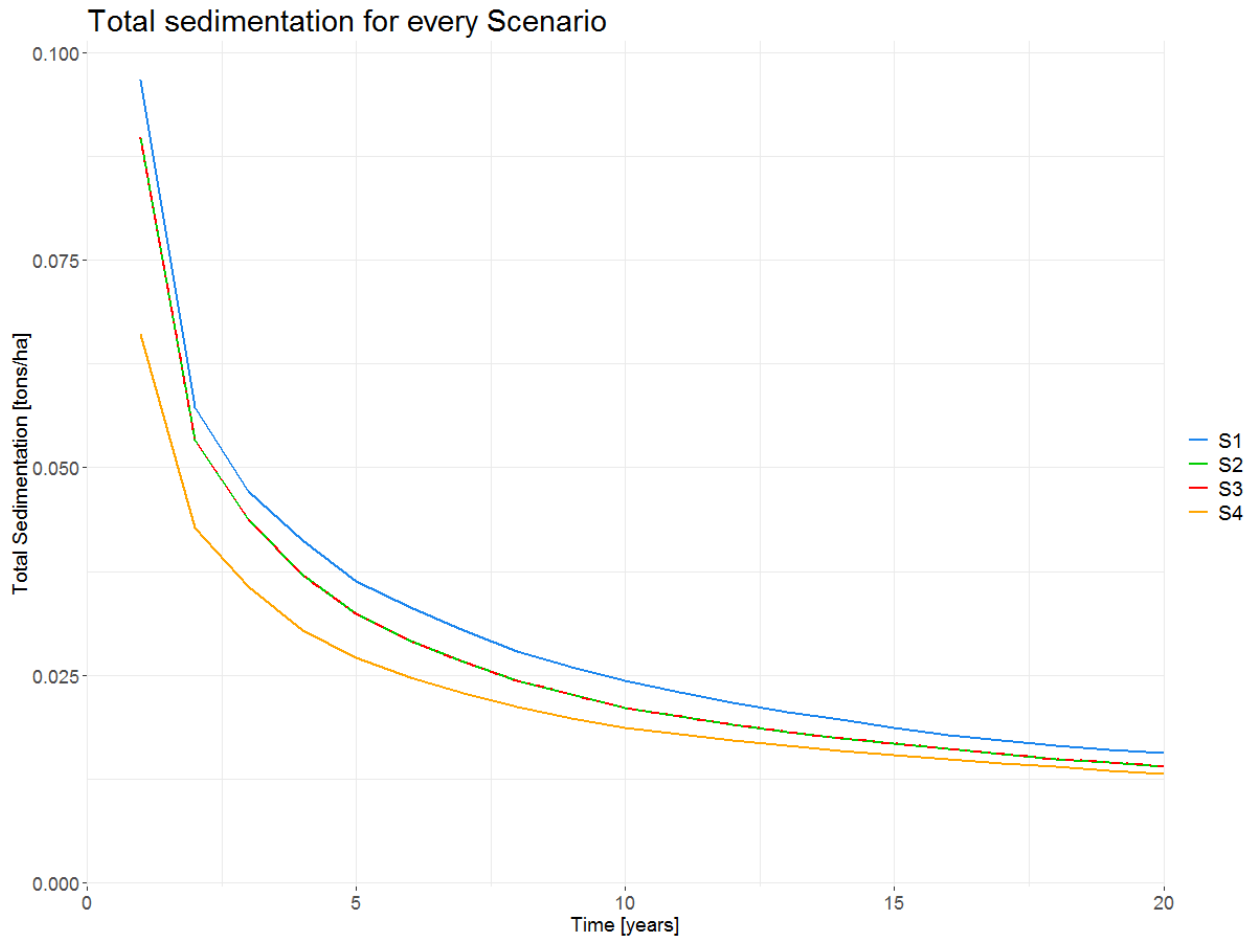


Figure 20 Total sedimentation for every scenario in the first 20 years. Unit is [tons/ha].

In Figure 21, the continuation of Figure 20 can be seen. The y-axis is adjusted to be able to better interpret the data. For every scenario, the total sedimentation shows strong variation in years 20 to 300, after which the sedimentation increases towards a relatively stable value at around 400 years. The same differences in magnitude between scenarios can be seen as in Figure 20. The total sedimentation in scenario 1 is relatively stable at around 0.022 tons/ha and the sedimentation in scenario 2 is relatively stable at around 0.018 tons/ha. The sedimentation in scenario 3 and 4 depict the same small-scale variation as in the erosion data visible in Figure 19. Every scenario except for scenario 4 shows two sudden drops in sedimentation around the years 3700 and 4000. The timing of these events are almost similar between every scenario, but not exactly similar. The magnitudes of the drops are similar, but not equal as well. The timing and magnitude of these drops in sedimentation are better visible in Figure 22, in which the difference in sedimentation per year is calculated. The sharp dips represent the drops in sedimentation visible in Figure 21. In Figure 22, it is visible that all scenarios but scenario 4 depicts the drops in sedimentation. The first dip is timed at the same year for every scenario and the second dip is only timed at the same year in scenario 2 and 3. The second dip is timed later in scenario 1. The magnitudes are similar

but not equal, as mentioned before. In both figures, it is clear that these drops in sedimentation do not occur in scenario 4, but the sedimentation remains at relatively constant magnitude with strong temporal fluctuations. In Figure 22 the fluctuations in the sedimentation in scenario 4 seems to have a certain pattern. This pattern starts with a sharp peak of increase in sedimentation after which a smaller decrease in sedimentation follows. This decrease in sedimentation slowly decreases to a certain point where a sharp peak again emerges. The timing and magnitudes of these fluctuations differ. After 5000 years the average total sedimentation of scenario 1 is 0.019 tons/ha/year and 0.015 tons/ha/year in scenario 2, 0.016 tons/ha/year in scenario 3 and 0.016 tons/ha/year in scenario 4.

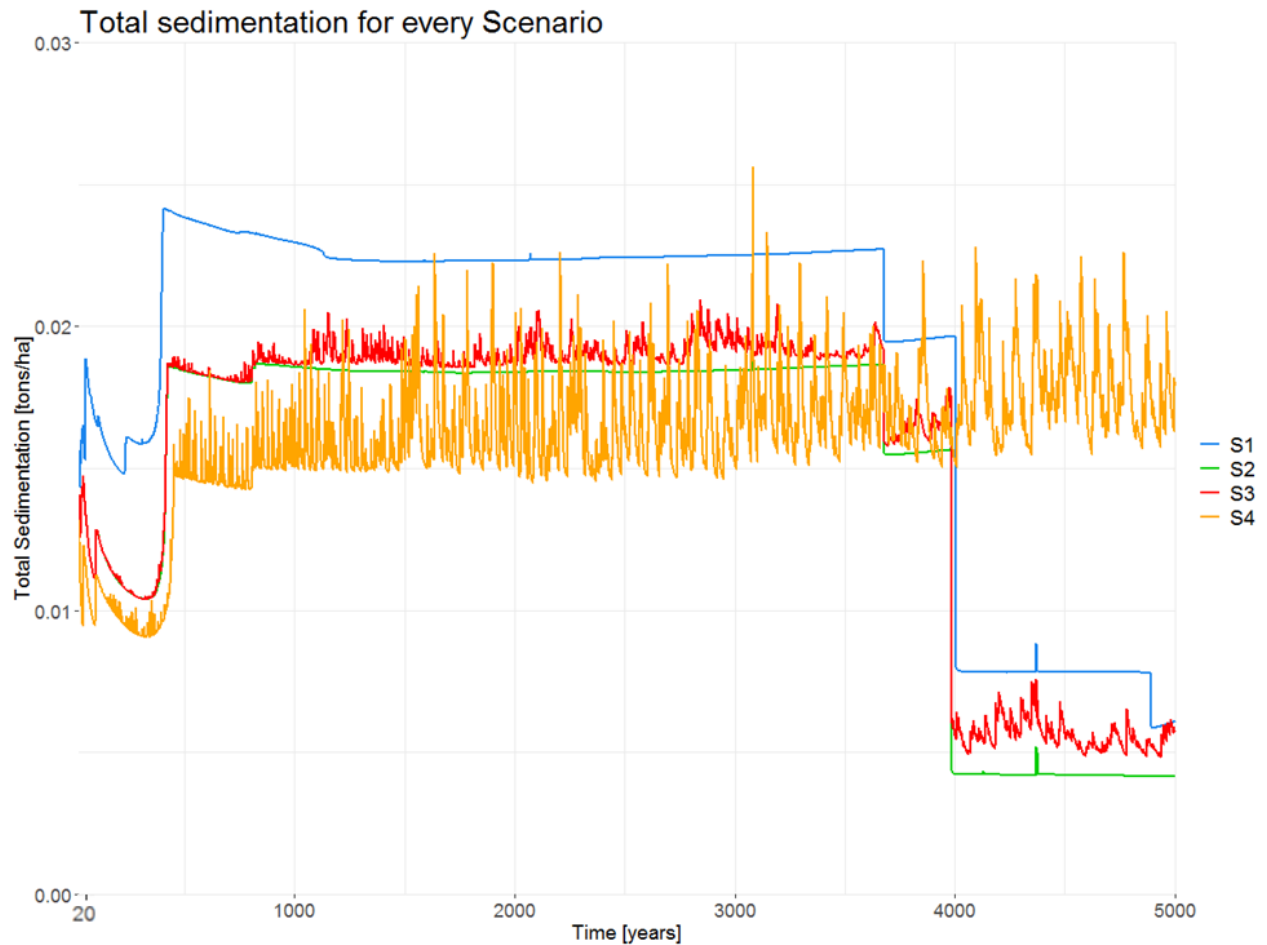


Figure 21 Total sedimentation for every scenario in years 20 to 5000. Unit is [tons/ha].

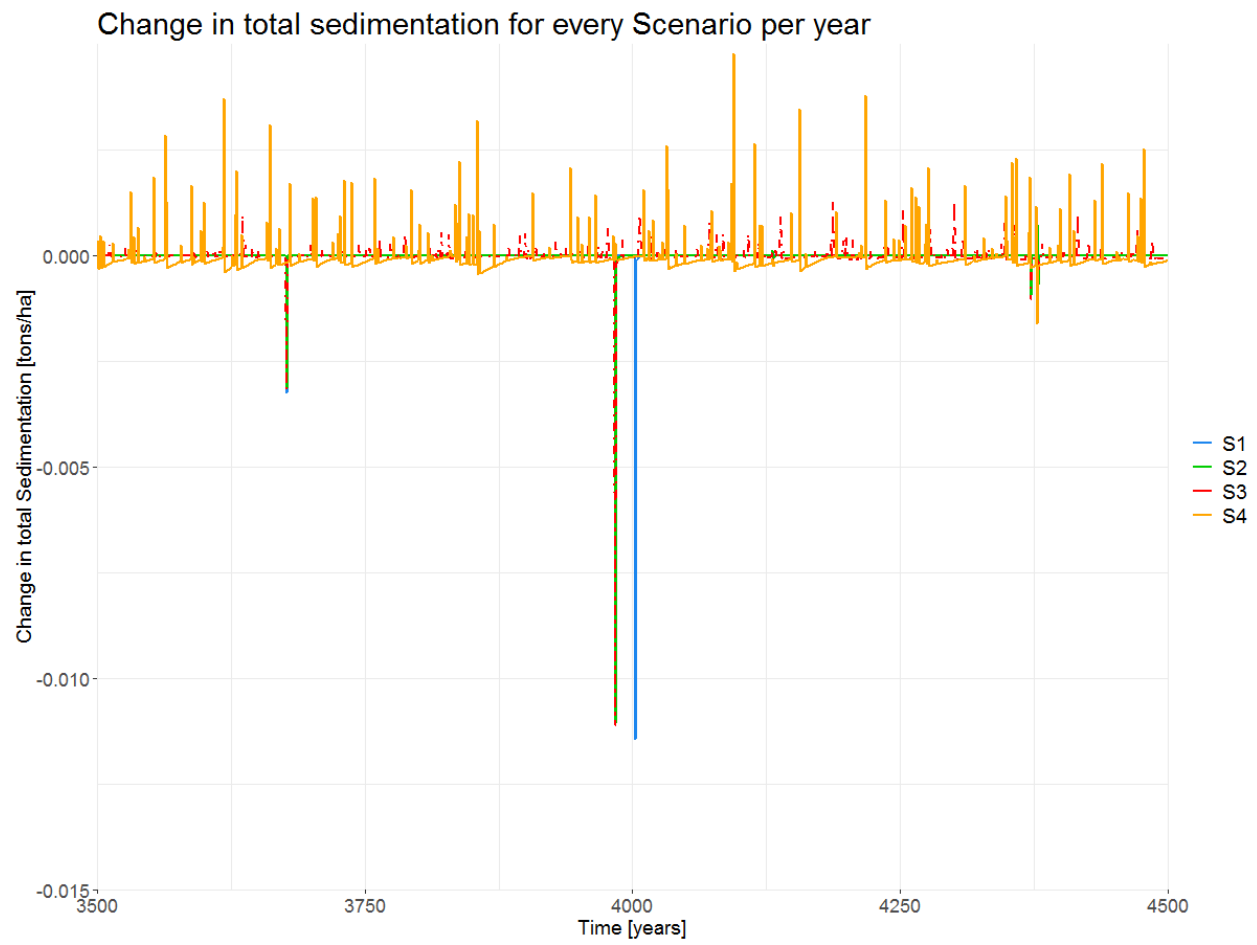


Figure 22 The change in total sedimentation for every scenario per year.

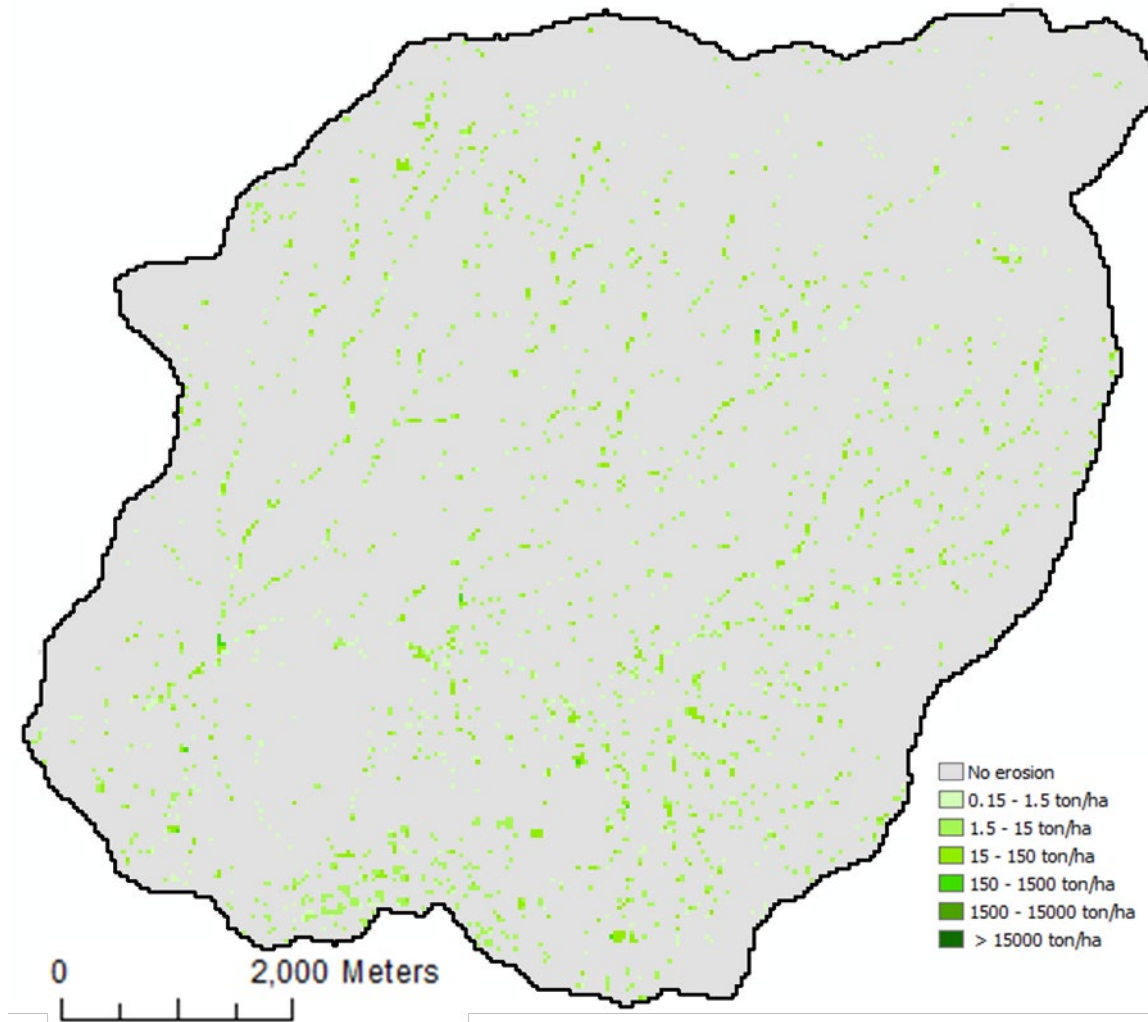


Figure 23 The sum of the total sedimentation in the first 20 years of scenario 3.

Figure 23 shows the sum of the total sedimentation in the first 20 years of scenario 3. It can be seen that in the first 20 years the sedimentation is much larger (Figure 20) and more widespread than later will be the case (Figure 21). The sum of erosion in the first 20 years in scenario 3 is 3 tons/ha, which is already almost 4% of the total sedimentation that will occur in the next 4980 years (78 tons/ha), while 20 years is only 0.4% of the total timespan of the full simulation. This difference in magnitude and location is consistent in all scenarios.

The differences in K-factor between scenarios can be seen in Figure 14. In Figure 24, the difference between the 5000 year DEM of scenario 2 and the 5000 year DEM of scenario 1 can be seen. In these configurations, erosion rates are many times higher than sedimentation rates, so it is relatively safe to assume that differences between scenarios are mainly caused by differences in erosion rates. In these configurations, erosion rates are many times higher than sedimentation rates, so it is relatively safe to assume that differences between scenarios are mainly caused by differences in erosion rates.

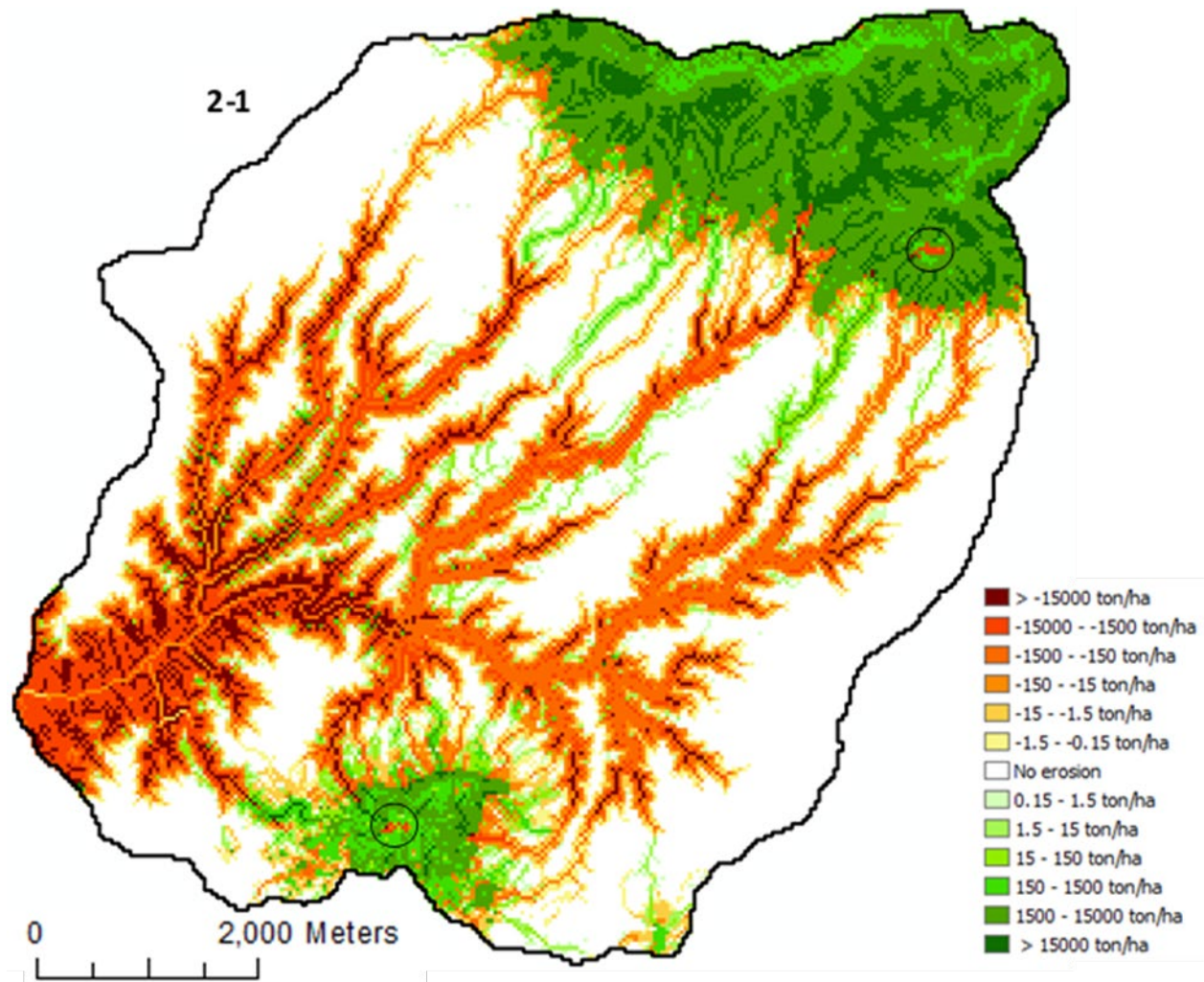


Figure 24 The difference between the 5000 year DEM of scenario 2 and the 5000 year DEM of scenario 1. The circled areas are deposition areas as can be seen in Figure 7.

A large decrease in erosion is visible in the limestone mountains in the north and on the basalt plateaus in the south of the badland area (Figure 24). Incision in the gully systems is stronger, apart from four systems close to the limestone mountains. In the lower part of the badland area, erosion is stronger around the centre of the gullies, whereas erosion is stronger in the centre of the gullies in the northern part of the badland area. At the border between the limestone mountains and the badland area, more incision has taken place. On the water divides and on the plateaus and ridges within the badlands, erosion amounts have not changed between scenarios. The circled red patches are deposition areas, as can be seen in Figure 18. This means that in this area a negative value indicates a decrease in sedimentation. The total erosion in 5000 years in scenario 1 is 61,000 tons/ha and the total erosion in 5000 years in scenario 2 is 59,500 tons/ha. The total sedimentation in 5000 years is 95 tons/ha in scenario 1 and 74 tons/ha in scenario 2.

In Figure 25, the 5000 year DEM of scenario 2 is subtracted from the 5000 year DEM of scenario 3. In scenario 3, the amount of erosion in the lower part of the badland area is lower than in scenario 2 and the amount of erosion in the centre of gullies is lower as well. The surrounding cells of the gully centres

however are more deeply incised. The limestone mountains and basalt plateaus were incised further upstream. The incision in the gullies close to the limestone mountains is less strong in scenario 3 with respect to scenario 2. The incision in the gully that incises the limestone mountain however, is much stronger in scenario 3. No change in erosion or sedimentation is visible on top of the limestone mountains or on the basalt plateaus. Just as the plateaus and ridges within the badlands and the water divides. This includes the deposition areas. The total erosion in 5000 years in scenario 3 is 70,000 tons/ha with respect to the 60,000 tons/ha in scenario 2. The total sedimentation in scenario 3 is 78 tons/ha.

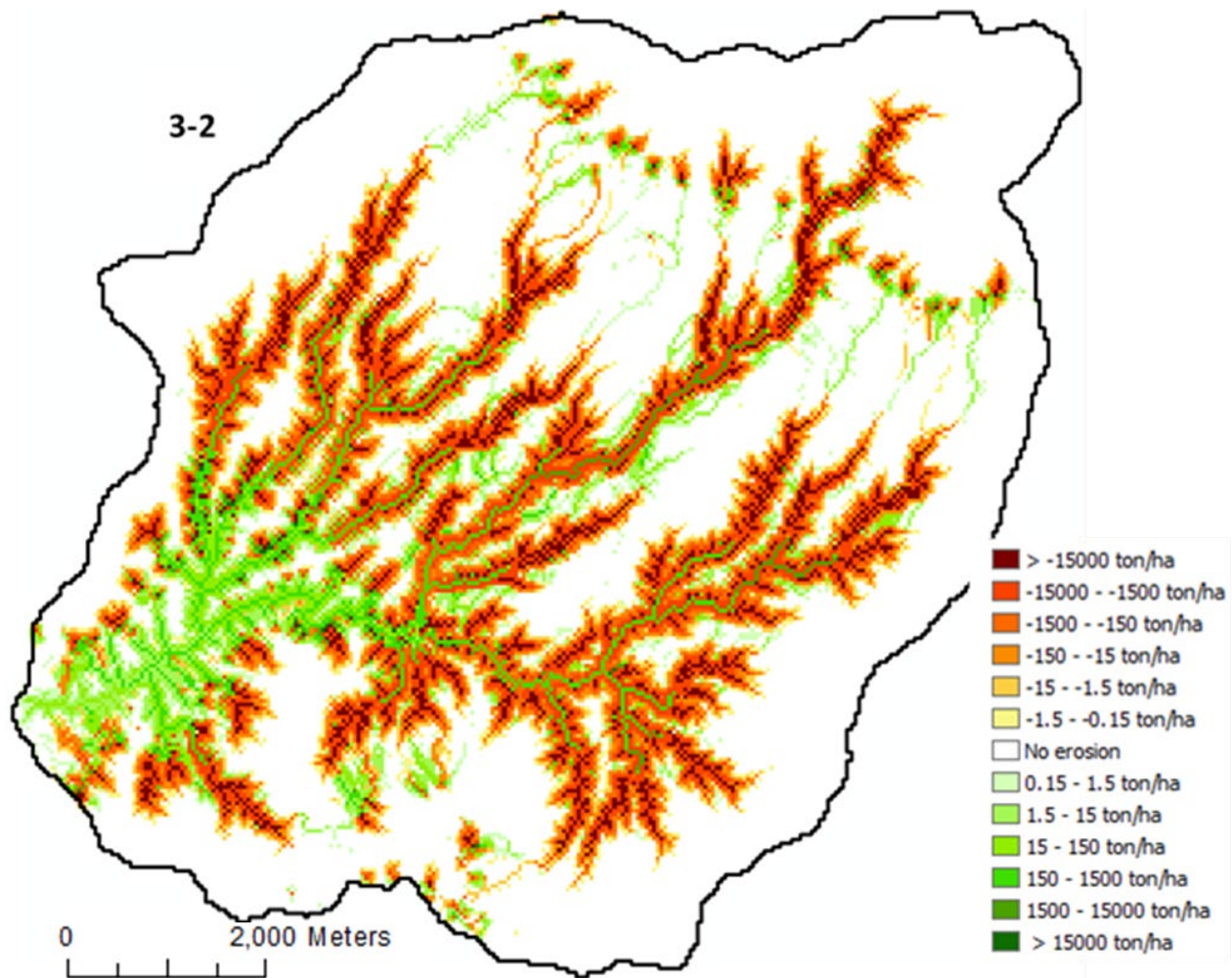


Figure 25 The difference between the 5000 year DEM of scenario 3 and the 5000 year DEM of scenario 2.

In Figure 26 the difference between the 5000 year DEM of scenario 4 and the 5000 year DEM of scenario 3 can be seen. Erosion rates in scenario 4 are higher in the lower lying area of the badlands and also higher in the centres of the gullies. The area surrounding the gullies in the low to middle altitude badlands, including the plateaus and ridges in the badlands, is prone to much less erosion with respect to scenario

3. The incision into the limestone mountains and into the basalt plateaus is lower as well. On top of the limestone mountains and basalt plateaus erosional processes are similar in both scenarios.

The total erosion in 5000 years in scenario 4 is 50,000 tons/ha with respect to the 70,000 tons/ha of scenario 3. The total sedimentation in scenario 3 is 81 tons/ha.

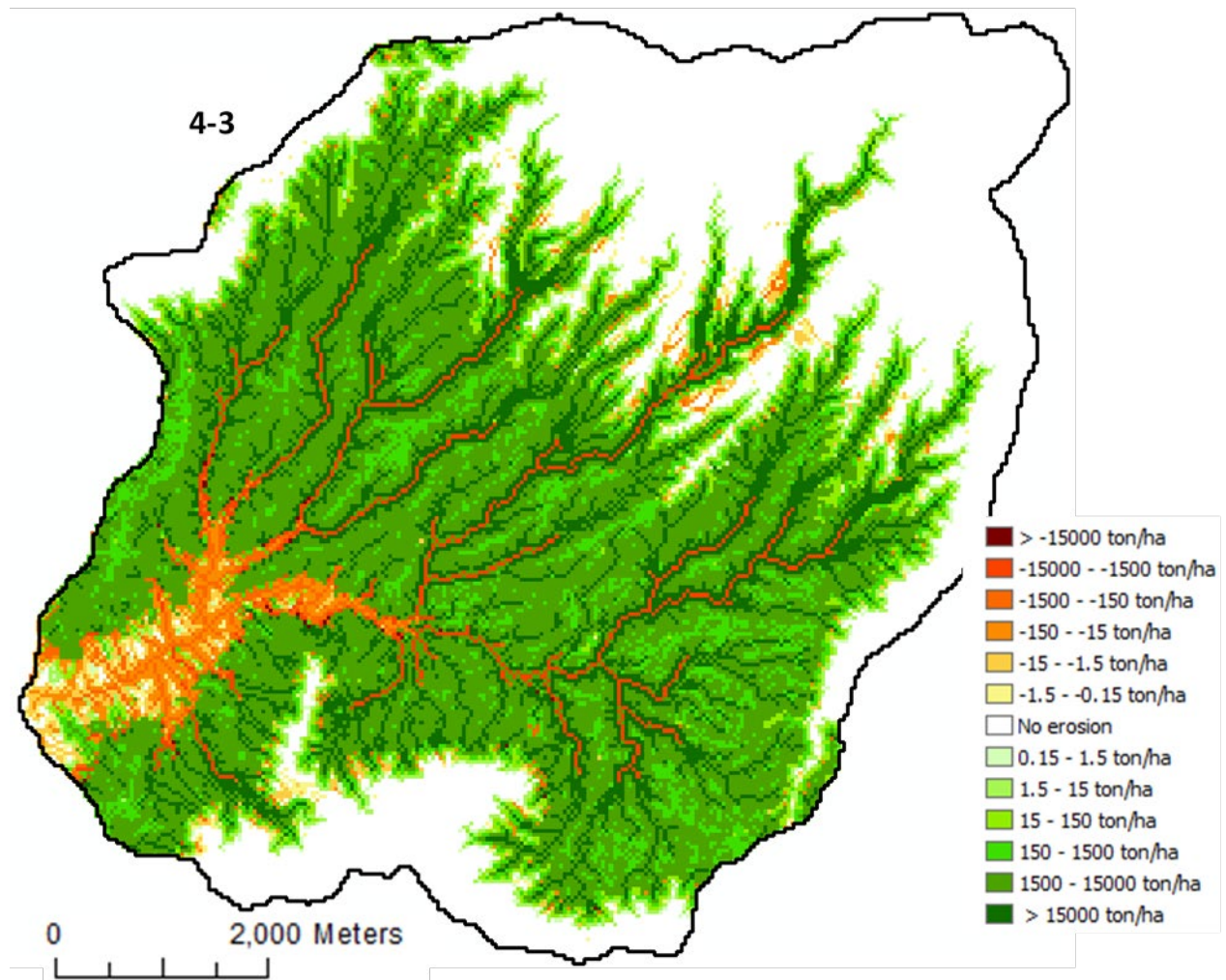


Figure 26 The difference between the 5000 year DEM of scenario 4 and the 5000 year DEM of scenario 3.

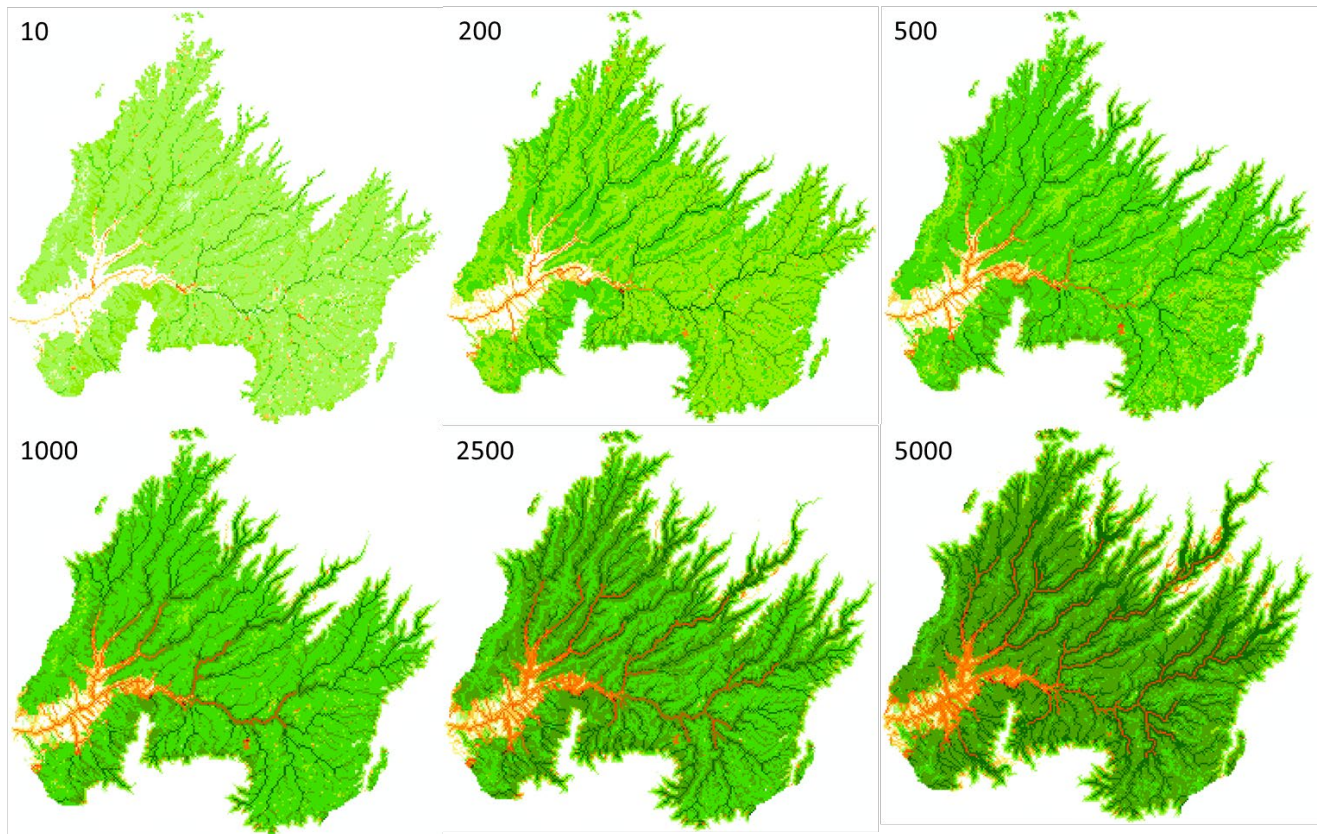


Figure 27 The difference between the DEM of scenario 4 and the DEM of scenario 3 in years 10, 200, 500, 1000, 2500 and 5000.

Figure 27 shows the difference in the DEMs of scenario 4 and 3 in the years 10, 200, 500, 1000, 2500 and 5000. In this time series it is visible that total erosion is at first lower in scenario 4 in the entire low badlands area, but after 200 years, the gully systems start to experience more erosion in scenario 4. This stronger erosion incision migrates increasingly upstream in the gully systems. Another phenomenon that is visible is the fact that the higher erosion in the lower badlands first starts in the gully systems, after which erosion becomes higher in the entire lower badlands area. These figures also suggest that the strong incision protruding in the limestone mountains is not as strong in the first 1000 years and is not as strong in scenario 4 with respect to scenario 3.

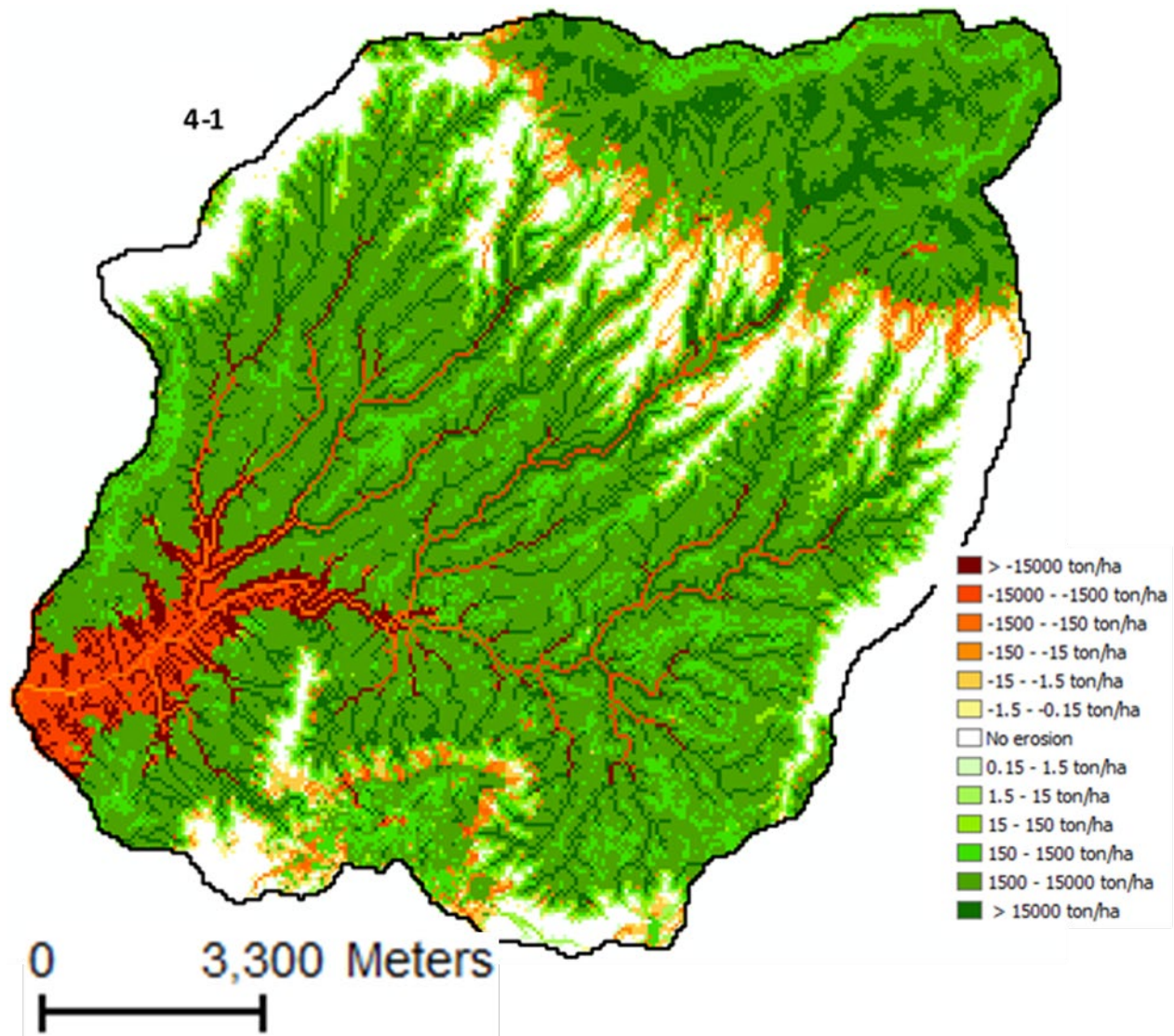


Figure 28 The difference between the 5000 year DEM of scenario 4 and the 5000 year DEM of scenario 1.

Figure 28 shows the difference between the 5000 year DEM of scenario 4 and the 5000 year DEM of scenario 1. It is visible that implementing different lithological units into the model changes erosional processes both spatially and in magnitude. Erosion is more local and extreme in the gully system, whereas overall erosion rates are limited. Incision into the limestone mountains and basalt plateaus is stronger, erosion on top of these mountains and platforms is less strong. Plateaus and ridges in the badlands areas are however mostly unaffected.

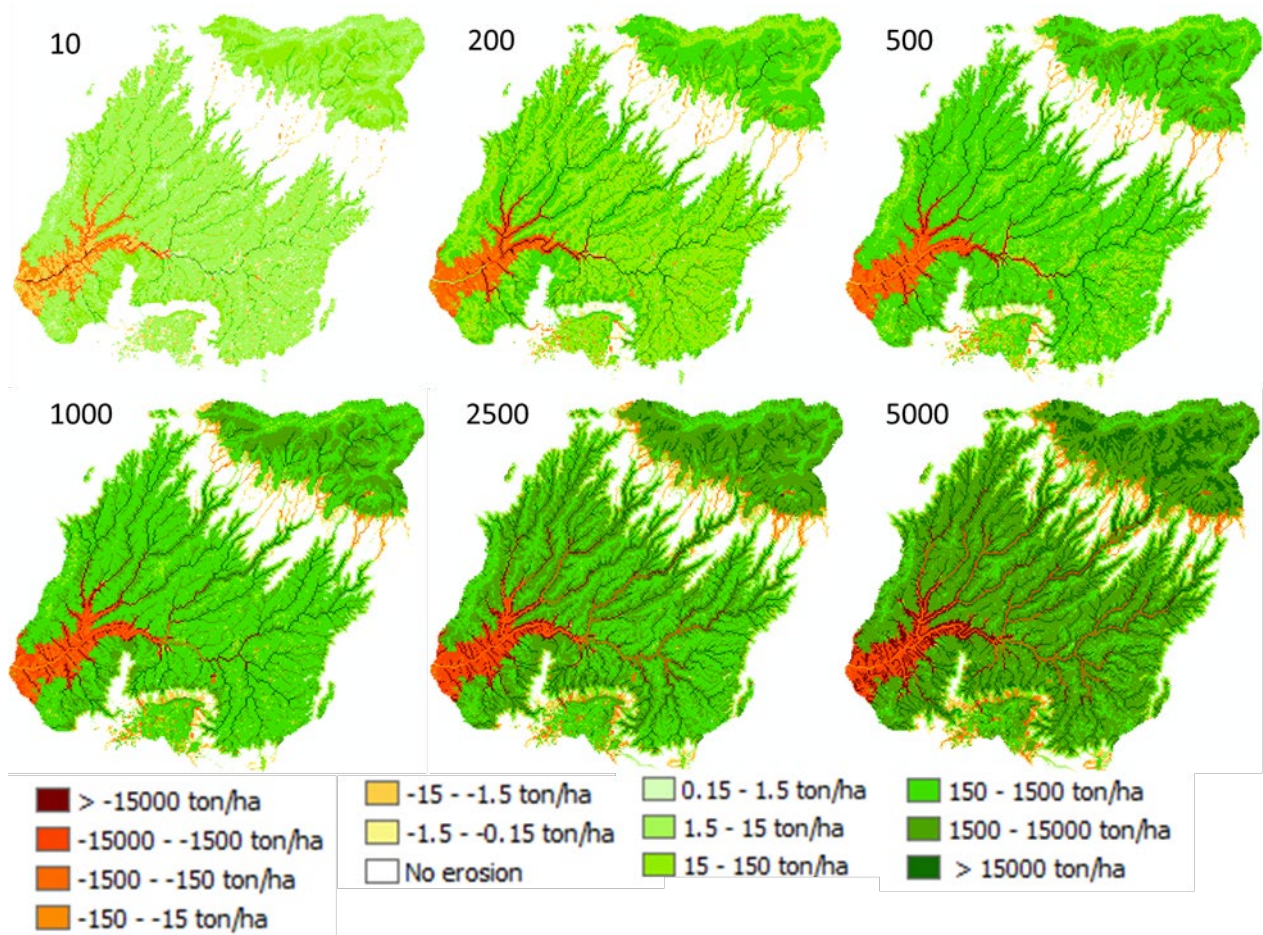


Figure 29 The difference between the DEM of scenario 4 and the DEM of scenario 1 in years 10, 200, 500, 1000, 2500 and 5000.

Figure 29 shows the difference between the DEM of scenario 4 and the DEM of scenario 1 in years 10, 200, 500, 1000, 2500 and 5000. It can be seen that incision in the upper badlands is higher in scenario 4 with respect to scenario 1. These erosion rates in scenario 4 in the limestone mountains and the basalt plateaus increase at a higher rate than the erosion rates in scenario 1. Erosion rates in the middle badland area, on the limestone mountains and on the basalt plateaus is increasingly lower with time in scenario 4. Critical incision into the gully systems in the middle badland area migrates increasingly upstream with time. Erosion rates in the lower badland area are increasingly higher in scenario 4 with time as well.

Figure 30 shows the difference in total erosion between scenario 4 and 1. As can be seen, in the first 500 years, erosion is higher in scenario 4, after which it decreases until a deficit of around 3 meters of erosion per year is reached.

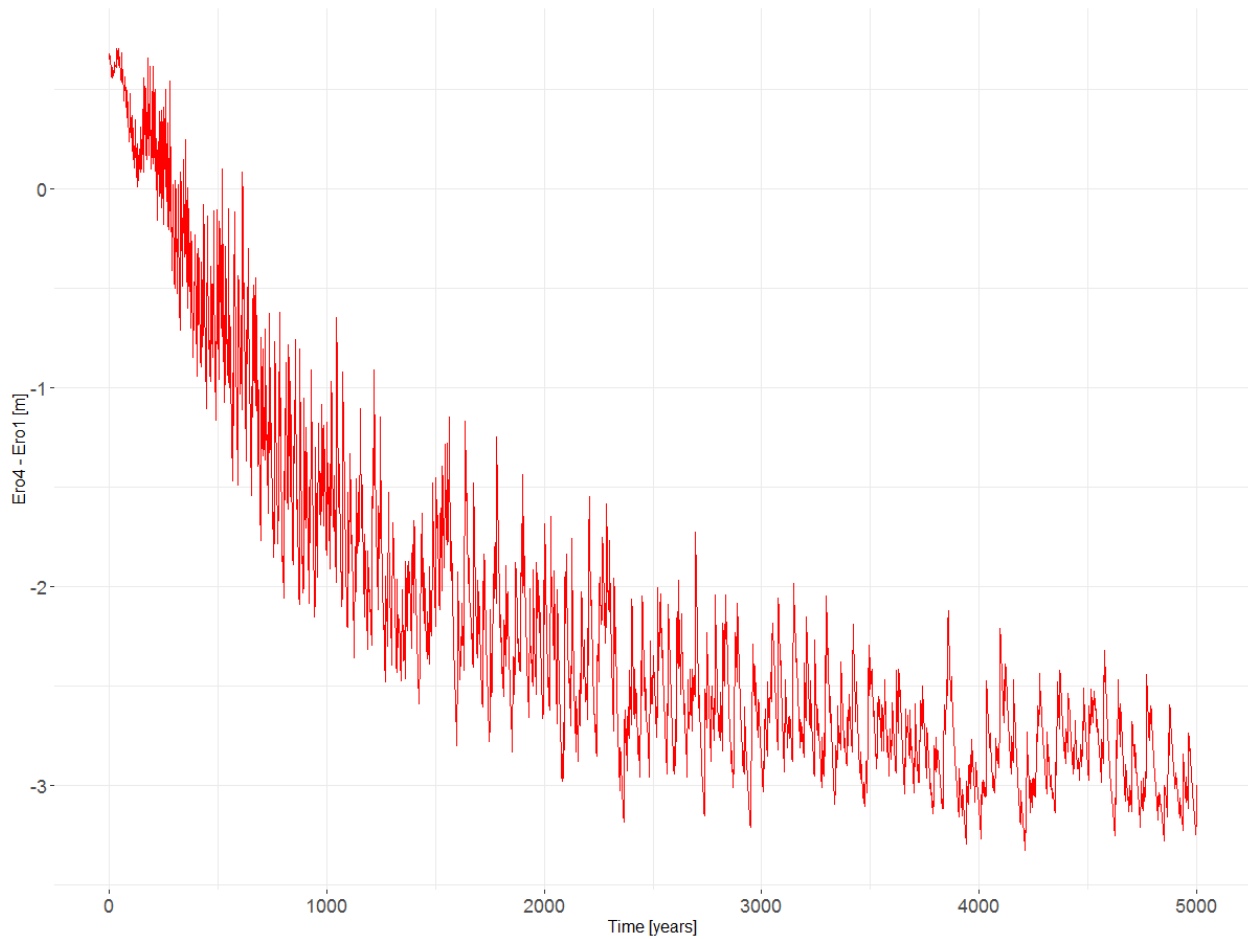


Figure 30 The difference between total erosion in scenario 4 and total erosion in scenario 1.

Local sedimentation

As discussed before, sedimentation seems to be rather local in the area. That is why sedimentation dynamics in the deposition areas indicated in scenario 1 will be examined in detail and compared with the entire research area. Figure 31 shows the local sedimentation in comparison with regional sedimentation. Local_sed1 (blue) represents the total sedimentation that took place only in the white circle number 1 that can be seen in Figure 18. Local_sed2 (green) and Local_sed3 (red) represent the total sedimentation in the other two circled areas. The total sedimentation of the entire area is represented in orange and the difference between the total sedimentation and the sedimentation in area 1 is depicted in grey. It can be seen that the sedimentation in area 1 is a very high fraction of the total sedimentation, on average 50% and between years 450 and 3750 around 65%. The first two dips in sedimentation that were discussed previously are situated in area 1 as well, a third dip at around year 4900 only visible in scenario 1 is situated in area 2. The total sedimentation in all three areas on average makes up for 92% of the total sedimentation in the entire area. In scenario 2, 3 and 4 these average percentages are 91%, 84% and 81% respectively.

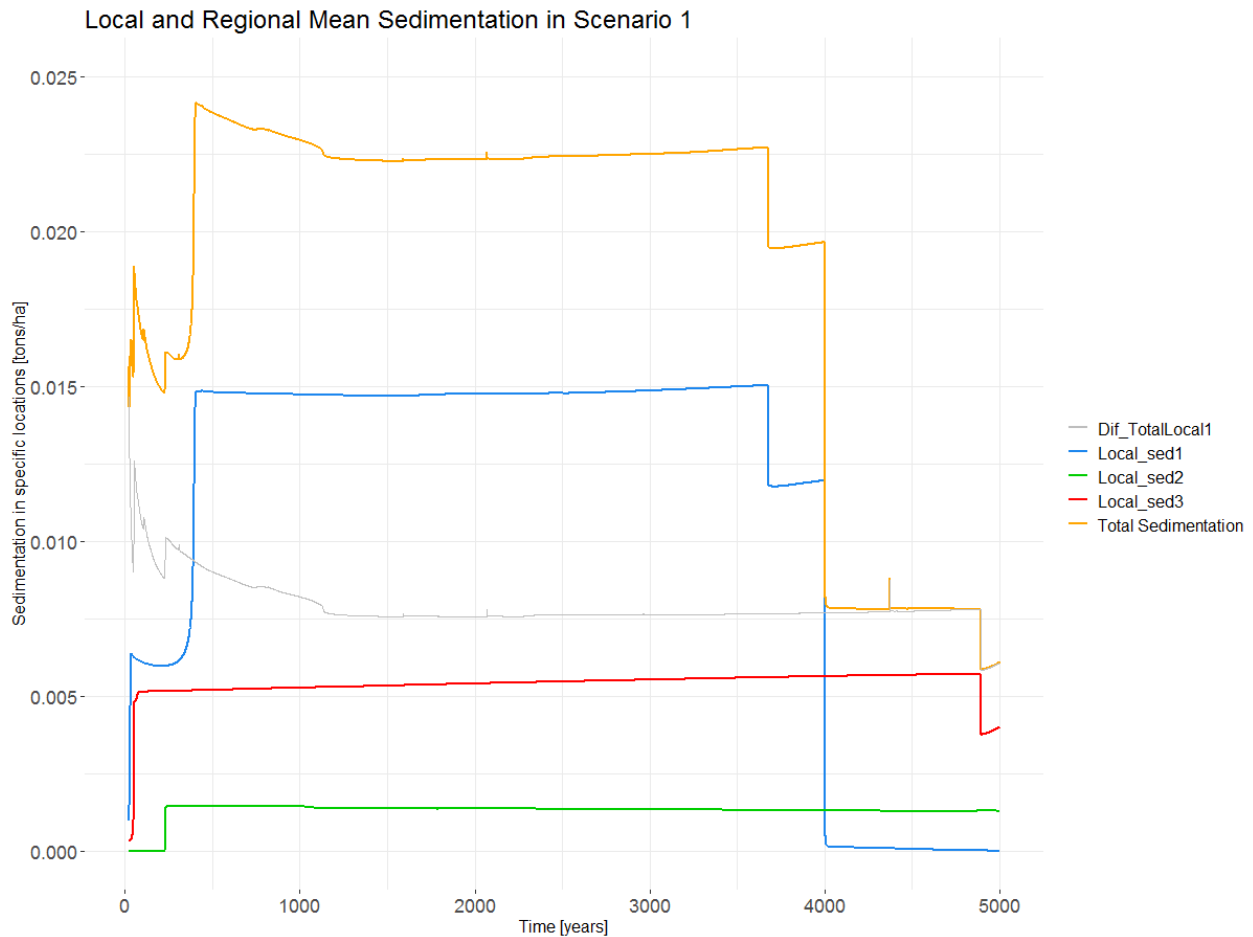


Figure 31 Local and regional sedimentation in scenario 1, the first 20 years are left out.

Lithological layer specific erosion and sedimentation

Figure 32 shows the calculations of the layers as defined in Figure 15. In scenario 1, the highest erosion rates are achieved in layer 3 (red), in which the erosion increases slightly with time. Erosion rates in layer 4 (yellow) are relatively high as well, but slightly decrease with time. Erosion rates in layer 2 (green) and 1 (blue) are relatively low (2 and 1.25 tons/ha respectively). In scenario 2, erosion rates are high in layer 4 (8 tons/ha), after which the erosion rates rapidly decrease in 350 years to 5 tons/ha. After this rapid decrease, the erosion decreases less strong and more constant. The total erosion in the layers 2 and 3 is relatively unchanged with respect to scenario 1. The total erosion in layer 1 is constant with time at 0.6 tons/ha which is twice as low than the erosion in layer 1 in scenario 1. In scenario 3, the erosion in layer 4 starts of high as well (8 tons/ha), but the decrease in erosion is much more gradual with time. Scenario 4 depicts the same dynamics, but the total erosion in layer 3 is much lower in comparison with scenario 3.

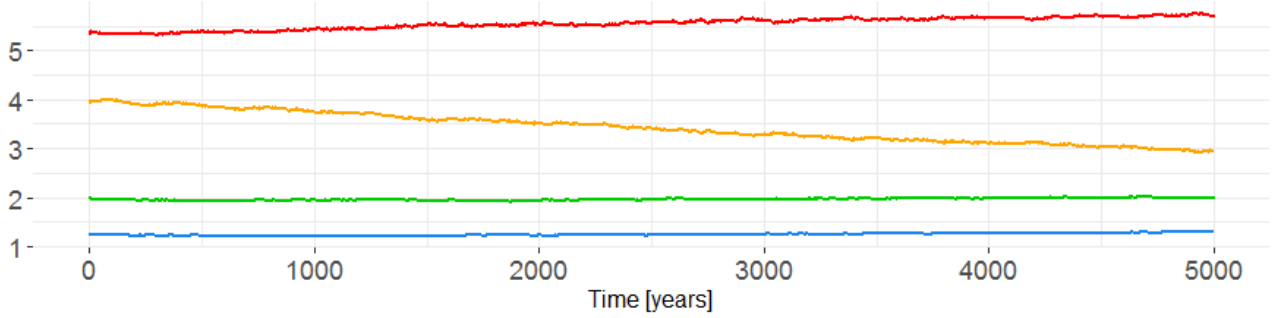
Figure 33 depicts the difference in total erosion within layers between scenario 2 and 1, between scenario 3 and 2 and between 4 and 3. The first graph shows that erosion in layer 2 and layer 3 almost do not differ between scenarios 2 and 1. Erosion in layer 4 is much higher in the first 350 years, as was mentioned before, after which the difference in erosion between scenarios is levelled out again. The erosion in layer

1 is somewhat lower in scenario 2 with respect to erosion scenario 1 (0.5 tons/ha). The second graph depicts the difference in erosion between scenario 3 and 2. The erosion in all layers start of at the same level, after which the erosion in both layer 3 and 4 becomes larger in scenario 3 with respect to scenario 4. Also visible are fluctuations in the difference in erosion in layers 1 and 2, which seem to be mirrored. In the third graph in Figure 33 it is visible that the erosion in layer 3 is much lower in scenario 4 compared to scenario 3. The erosion in layer 4 starts equal in both scenarios, but then the magnitude of total erosion decreases faster in scenario 4 than in scenario 3.

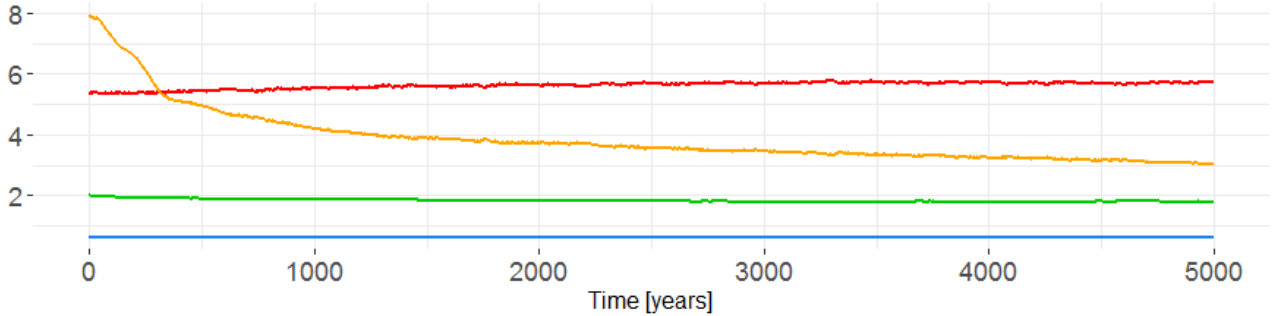
Figure 34 shows the lithological layer specific total sedimentation in every scenario. Total sedimentation in scenario 1 draws some attention, since at around 1900 years, the sedimentation in layer 3 seems to decrease at which time sedimentation in layer 4 increases. The same seems to happen in scenario 2. However, there is more noise in the data in this case. In scenarios 3 and 4, sedimentation in layer 3 hardly drops at this 1900 year point and sedimentation in layer does not significantly increase.

In every scenario the largest amount of material is deposited in layer 3. At around 4000 years, sedimentation drops in both layer 3 and 4 in the first two scenarios. In scenario 3, sedimentation only drops in layer 3 and the sedimentation does not drop in any layer in scenario 4.

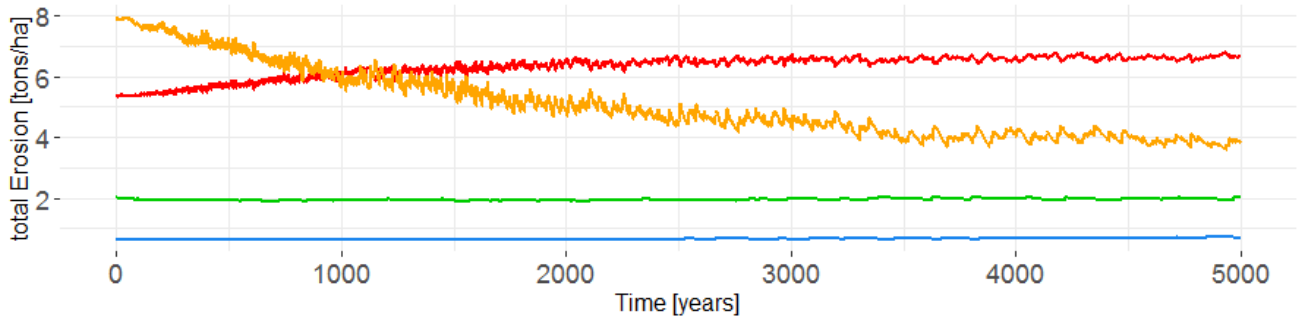
Total Erosion for scenario 1 per lithological layer.



Total Erosion for scenario 2 per lithological layer.



Total Erosion for scenario 3 per lithological layer.



Total Erosion for scenario 4 per lithological layer.

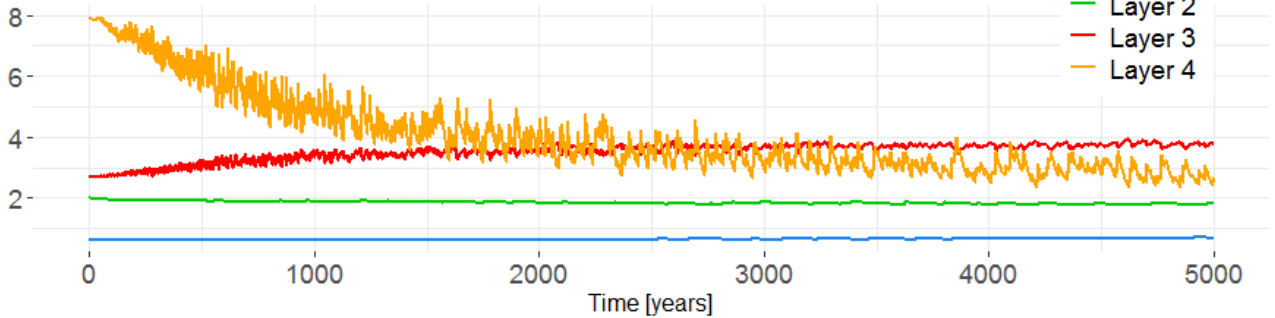


Figure 32 Lithological layer specific total erosion in every scenario.

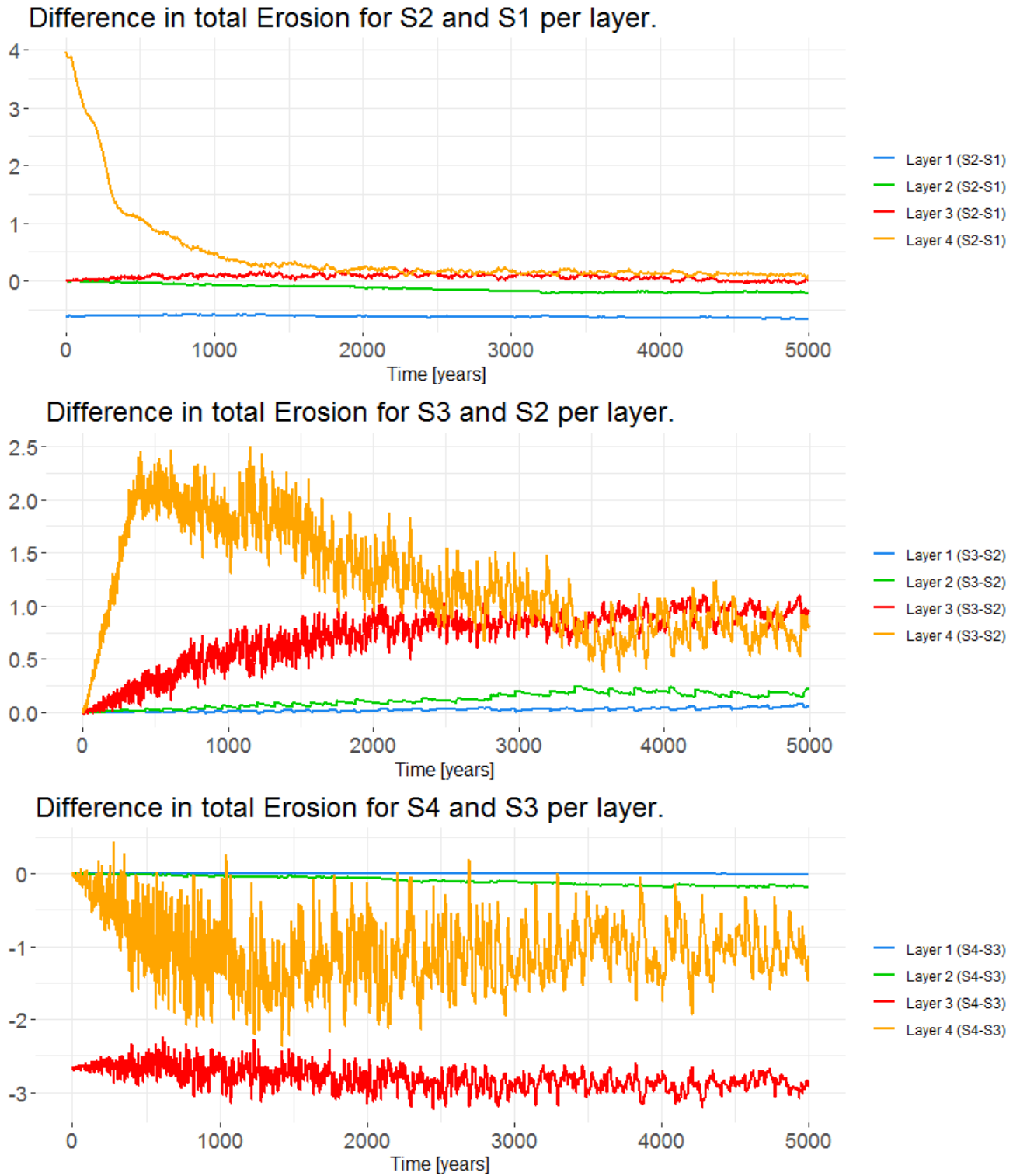


Figure 33 Difference in total erosion within a layer between scenarios.

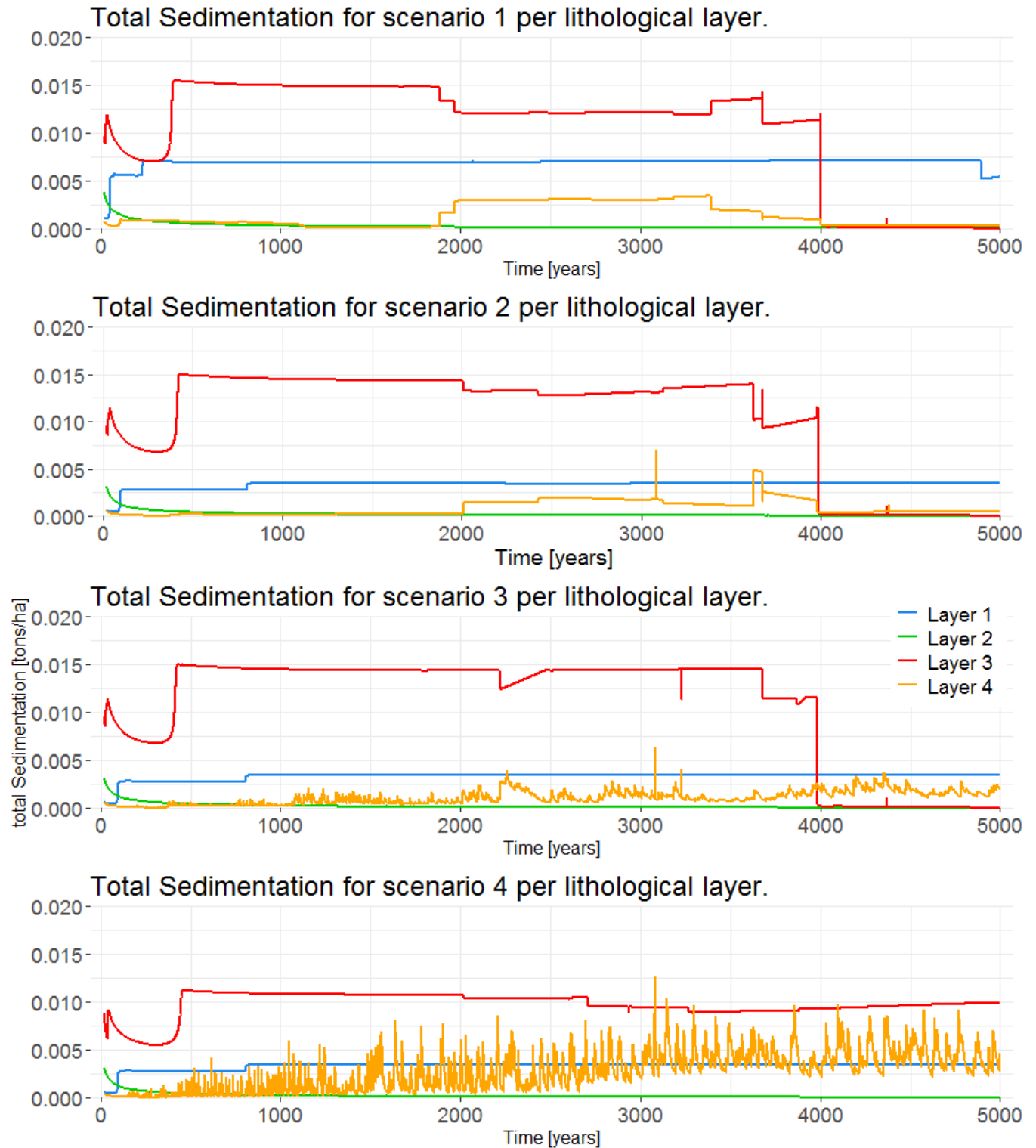


Figure 34 Lithological layer specific total sedimentation in every scenario, the first 20 years are removed from these time series.

Discussion

As can be seen in Figure 18, the largest amounts of erosion take place in erosion gullies. This distribution indicates that, apart from the effect of lithology, the gullies are the most erosion prone areas from a topographical point of view. In these areas gradients are strongest and erosional dynamics are more active.

Furthermore, total sedimentation is small and local over 5000 years. Although, in the first 20 years sedimentation is rather large and regional (Figure 20). As can be seen in Figure 23, sedimentation occurs in most of the gully systems. This indicates the model redistributing and smoothing the gully landscape. At some point, in this case after around 20 years, the landscape is smoothed in such a way that no more grids are available for sedimentation in the gully systems due to the gradient distribution or due to the sediment loading. In this case erosion rates are relatively stable, so the filling progress in gully systems is mainly stopped because of gradient distribution, meaning that slopes are either too steep for sedimentation, or the system experiences sediment hunger. Sediment hunger indicates unsaturated sediment capacity in the water flow in the system.

In Figure 19, the total erosion time series of every scenario can be seen. The change from scenario 1 to scenario 4 in K-factor is expressed in the erosion output by a high erosion rate from the beginning of the configuration of scenario 2. This is due to the higher K-factor in the lower part of the badlands, as can be seen in Figure 14.

Figure 24 shows the spatial difference between scenario 2 and 1. As mentioned before, erosion rates are higher in the lower badlands and lower in the limestone mountains and on the basalt plateaus. This is reasonable, since the K-factor was changed in a similar way. What is interesting to see however, is the change in erosion rates in the middle and higher part of the badlands. The K-factor is not altered in these areas, but the erosion rates are different. In this case it is caused by changes in saturation of the carrying capacity of the water flow. Because of the relatively limited amount of erosion in the limestone mountains and on the basalt plateaus, the water carries less material when entering the badland gullies. The system in this area becomes detachment limited. This means that the capacity is less saturated, increasing the potential for erosion. This also means that the badlands are topographically suitable to fulfil this increased potential to some extent. The total sedimentation in the deposition areas marked in Figure 18 and Figure 24, is lower in the case of the basic lithological layers in scenario 2 with respect to the base scenario in scenario 1. This is due to the fact that less material is available in the water flow, because of lower erosion rates in the limestone mountains and on the basalt plateaus.

Figure 25 shows the spatial difference between scenario 3 and 2. The initial K-factor distribution is similar in both scenarios, but incision into a different lithological layer is possible in scenario 3. What can be seen is that erosion rates are lower at the boundaries between lithological layers. When the area north of a boundary is incised, a different lithological layer with a higher K-factor is reached relatively quickly. This leads to higher erosion rates at these locations, which will result in less erosional power downslope of the K-factor boundaries. This is why erosion rates are lower in the upper badlands and in the lower badlands.

The possibility of incision into different lithological layers in scenario 3 creates a situation in which the model is much better able to redistribute the topography of the badlands. Figure 19 shows that erosion rates stay higher much longer with respect to the basic lithological layers in scenario 2. As mentioned before, small-scale variations in both erosion and sedimentation rates occur (Figure 21). These variations indicate constant redistribution of materials, which occur due to the fact that the model can continue finding new areas to erode into. The total amount of erosion is therefore much higher when adding incision based K-factor change (70,053 tons/ha) with respect to the basic lithological layering (59,658 tons/ha).

Figure 26 shows the spatial difference between DEMs of scenario 4 and 3. The middle badlands experience much less erosion, except for the gully systems. The K-factor is lower in this scenario, which causes the decrease in erosion. This phenomenon does however strengthen the incision into the gullies, which is caused by the more detachment limited surroundings. The incision in the lower badlands is increased because of the same reason. In Figure 26 it can be seen that the amount of erosion is lower in the entire middle badlands, even in the gully systems, in the first 200 years. However, when a new lithological layer is incised, the K-factor changes and extreme erosion takes place in the incising gullies. This critical incision migrates upstream with time.

As mentioned in the results section, the extending incision into the limestone mountains is less strong in scenario 4 in comparison to scenario 3. This is again because of the K-factor distribution. As can be seen in Figure 27, incision into the limestone mountains will first result in a higher K-factor, but incision into the following rock/sedimentary unit will result in a lower K-factor. This influences the sediment load of the water flow and thus changes the dynamics of erosion and sedimentation downstream as well.

Total erosion in the lower badlands area is higher in scenario 4, because of the detachment limited middle badlands area. However, as can be seen in Figure 27, this increase in erosion begins in the main gully system and only later does it affect the smaller side gullies.

To summarize the spatial effect of lithology on erosional processes and landscape evolution, Figure 29 shows the total difference between scenario 4 and the base scenario. This figure shows how erosion is forced to occur very locally because of detachment limitations in the limestone mountains, the basalt plateaus and the middle badland area. At the borders between lithological units, erosion is higher. This is where the transport capacity of the water flow can be fulfilled. The figure also shows that incision into the gullies is very strong and that this strong incision migrates upstream with time. After 5000 years, a clear difference in distance of migration between gullies is visible. This indicates differences in catchment area (water availability), erosional susceptibility and topographical profile between gullies.

The upper parts of plateaus and ridges within the badlands are hardly affected by the effect of lithology. This might explain a part of the existence of these plateaus. It is a striking feature in the landscape and still not clear how these plateaus still exist. Based on the results of this thesis, spatially dominant erosion, which eludes these platforms, might be a part of the reason of their existence. Vertical incision is much stronger than horizontal sideways, lateral erosion carving in this area. This effect is magnified by the application of lithology, which is also visible in Figure 28. As suggested by Forte et al., (2016), landscapes that accommodate less erodible rocks will develop a less dense drainage system with deeper incisions in comparison with higher erodible landscapes. This phenomenon also plays a role in creating the results of

these simulations. Also, spatial variation in erodibility might result in knickpoint creations at the border of two lithological units (Haviv et al., 2010). However, both of these phenomena are mostly frequent in solid bedrock landscapes and not in sedimentary rocks that are investigated in this thesis. Still, the influence of the lithologies in this area seems to recreate these phenomena to some extent.

Total sedimentation in the first 20 years can be seen in Figure 23. This figure explains the relatively high sedimentation amounts in the first 20 years of every simulation. The LAPSUS model will try to configure the landscape in the sense that the topography will be smoothed out in the first period of a simulation. All the grid cells in the DEM that are fit locations for sedimentation are filled, after which the amount of sedimentation locations is limited. This is not the result of model instability, but can be interpreted as a start-up period. After this period, only three small patches experience net sedimentation. Two of these locations are on flat surfaces on the limestone mountains (number 3 in Figure 18) and the basalt plateaus (number 2 in Figure 18). The other area (number 1 in Figure 18) is located somewhat upstream in a gully system. These locations have much potential for sedimentation and are slowly filled with material. At 3700 years, some cells are filled and the sedimentation area migrates somewhat more upstream. At 4000 years, the cells are completely filled and no longer have a capacity to hold any more material. This is where total sedimentation is decreased notably. In the field, deposition areas seem to be more common and it is not expected that sedimentation would mostly stop after 20 years. In Schoorl et al., (2014) sediment waves in LAPSUS modelling are discussed in the Sabinal catchment, Andalusia, Spain. Sediment waves are defined as alternating zones of erosion and deposition that migrate along the longitudinal profile over time (Figure 35).

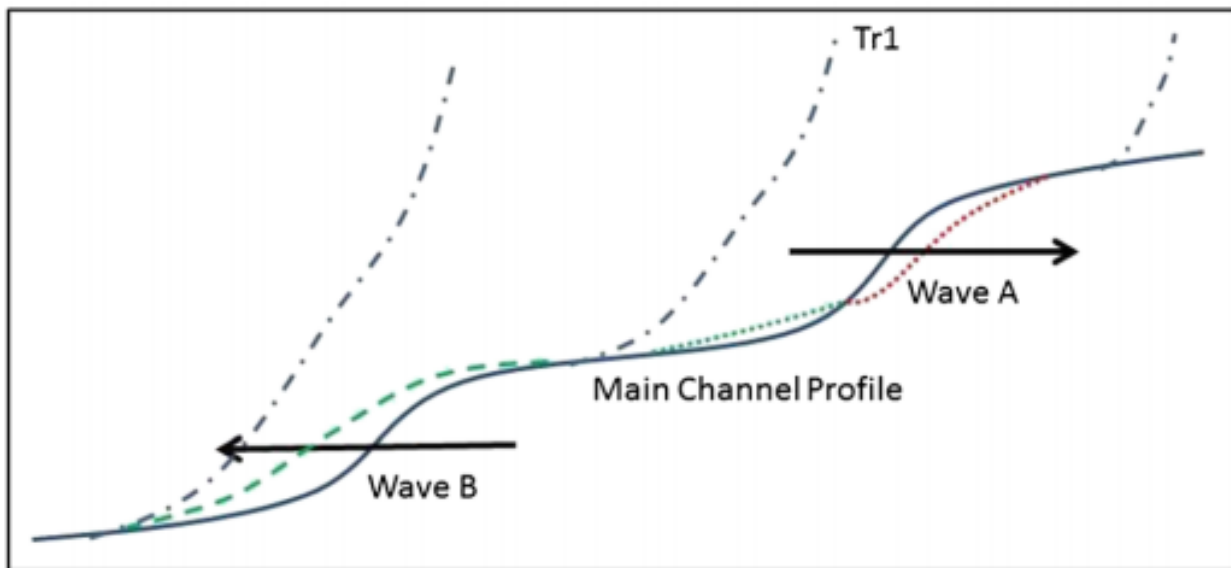


Figure 35 Conceptual drawing showing the main channel, with incoming tributary (Tr1) and two sediment wave systems with Wave A as the headward erosion sedimentation system and Wave B the downstream pro-gradation sediment lobe system. (Taken from (Schoorl et al., 2014)).

In the results of this modelling research, it seems that only migrating erosional waves occur, and the downstream migrating deposition is lacking. This might be because of the fact that there are simply no locations suitable for sedimentation in this area, or because of the detachment limited surroundings of the gullies. These might be limiting the sediment load to such an extent, that the migrating erosional wave still does not satisfy the sediment load. The water is not filled with sediments to its full potential, and downstream erosion continues. This does not seem to be a natural occurring phenomena and this might indicate that the erodibility differences between the lithological layers are too high for this area.

Erosion increases in layer 3 and decreases in layer 4 at the same rate in the base scenario, as can be seen in Figure 32. The same can be seen in a landscape with basic lithological layers, only with a higher total erosion in the bottom layer. This increase and decrease resembles the upstream migration of erosion, together with the upstream migration of the border between lithological units. The difference between the scenarios is visible in Figure 33. Total erosion in layer 1 is higher in the base scenario with respect to the basic lithological layer scenario, which is caused by a higher K-factor. When erodibility can be changed by incision, erosion rates in layer 3 decrease at a lesser rate. Which is caused by the higher flexibility of the landscape. With flexibility, a higher capacity of rearranging material because of a higher K-factor flexibility is meant.

As can be seen in Figure 17, the lithological distribution in the area is more complex than was modelled. Even lithological units themselves are not uniform, like the upper badland materials. Even after using a simplified version of the stratigraphy, a large effect of the lithological difference on erosion dynamics is modelled. This is only a small portion of the actual effect of the lithology in this area. If the actual lithology would be implemented in the numerical modelling, the influence of spatial and quantitative erosional dynamics of the area would be higher.

The effect of lithology is one of many factors influencing landscape evolution in this area. Tectonic regimes (Garcia-Castellanos & Villaseñor, 2011), land use (Van Rompaey et al., 2002), climate change (Lavee et al., 1998), base level change (Doré & Jensen, 1996) and volcanic events (Maddy et al., 2012; van Gorp et al., 2013) might have major influences on erosional processes as well. Conclusions drawn from this thesis must always be interpreted as a part explanation of a larger and more complex system.

The results of this thesis must be carefully interpreted because of the lack of good calibration and validation data and the lack of solid age control measurements. Validation of spatial landscape evolution models is considered problematic because of the difficulty of obtaining spatial validation data (Jetten et al., 2003). The effect of DEM resolution is also very strong and should not be forgotten (Schoorl et al., 2000). The erosion and sedimentation quantities are not to be trusted completely. However, the spatial dynamics and relative quantitative differences still provide trustworthy and valuable information on landscape evolution.

Mitchener & Torfs (1996) describe the effect of differences in mud/sand mixtures on erosion rates. They indicated that increasing or decreasing mud fractions in sediments affects erosion rates significantly. This further showcases the possible effect of different lithological units on erosion rates. Also, sediment load and grain size greatly influence incision rates spatially and in magnitude, as was found by Sklar & Dietrich (2001).

Conclusions

From the data gathered in the field, the sediments and stratification of the badland area could be mapped on a fairly high detail. The interpretation of the lithology of the area provided a solid basis for landscape evolution modelling scenarios. Five dominant depositional units were identified in the field which were translated into four different erodibility layers based on erodibility estimations for modelling with LAPSUS. The K-factor distribution was defined from top to down respectively 'low' ($1.23 \cdot 10^{-5}$), 'normal' ($2.47 \cdot 10^{-5}$), 'low' and 'high' ($4.94 \cdot 10^{-5}$).

Lithology influences erosion dynamics in the badland area both spatially and in magnitude. Adding simplified stratification to the LAPSUS model causes high incision rates at boundaries between lithological units. This is due to detachment limited upstream limestone plateaus and basalt plateaus. Adding the possibility of incision into different lithological layers creates a situation in which the model is much better able to redistribute the topography of the badlands. At first, the spatial variation in K-factor distribution causes low incision rates in the main badland area. However, after 500 years, an incision pulse in the main gullies begins on the boundary between lower badlands and middle badlands. This pulse causes high erosion rates and spatially very narrow erosion patterns in the main gullies and migrates upstream into the higher badlands in a time span of 5000 years. The presence of lithology causes steeper slopes and, in this case, lower overall erosion rates. The model's capacity of redistribution of material (erosion and sedimentation) in the landscape is increased. Side gullies are less active and plateaus and ridges in the badlands are mostly unaffected. This combination of results gives an indication of a possible cause for the preservation of these plateaus. The model is better capable of redistributing erosional locations, due to a more dynamic erosional surface. The results of these modelling exercises stress the importance of understanding the stratigraphy of an area for interpreting landscape evolution and erosional processes. This effect should not be easily discarded in general, and in the case of the badland area, should be taken into account as very significant.

References

- Brandolini, P., Cevasco, A., Capolongo, D., Pepe, G., Lovergine, F., & Del Monte, M. (2018). Response of Terraced Slopes to a Very Intense Rainfall Event and Relationships with Land Abandonment: A Case Study from Cinque Terre (Italy). *Land Degradation and Development*, 29(3), 630–642. <http://doi.org/10.1002/ldr.2672>
- Bryan, & B., R. (1978). Factors controlling the initiation of runoff and piping in Dinosaur Provincial Park badlands, Alberta, Canada. *Zeit. Geomorph. N. F., Suppl. Bd.*, 29, 151–168. Retrieved from <http://ci.nii.ac.jp/naid/10003515838/en/>
- Cantón, Y., Domingo, F., Solé-Benet, A., & Puigdefábregas, J. (2001). Hydrological and erosion response of a badlands system in semiarid SE Spain. *Journal of Hydrology*. [http://doi.org/10.1016/S0022-1694\(01\)00450-4](http://doi.org/10.1016/S0022-1694(01)00450-4)
- Cantón, Y., Solé-Benet, A., & Domingo, F. (2004). Temporal and spatial patterns of soil moisture in semiarid badlands of SE Spain. *Journal of Hydrology*, 285(1–4), 199–214. <http://doi.org/10.1016/j.jhydrol.2003.08.018>
- Cyr, A. J., & Granger, D. E. (2008). Dynamic equilibrium among erosion, river incision, and coastal uplift in the northern and central Apennines, Italy. *Geology*, 36(2), 103–106. <http://doi.org/10.1130/G24003A.1>
- Doré, A. G., & Jensen, L. N. (1996). The impact of late Cenozoic uplift and erosion on hydrocarbon exploration; offshore Norway and some other uplifted basins.; Impact of glaciations on basin evolution; data and models from the Norwegian margin and adjacent areas. *Global and Planetary Change*, 12(1–4), 415–436.
- Ersoy, Y. E., Helvacı, C., & Sözbilir, H. (2010). Tectono-stratigraphic evolution of the NE-SW-trending superimposed Selendi basin: Implications for late Cenozoic crustal extension in Western Anatolia, Turkey. *Tectonophysics*. <http://doi.org/10.1016/j.tecto.2010.01.007>
- Forte, A. M., Yanites, B. J., & Whipple, K. X. (2016). Complexities of landscape evolution during incision through layered stratigraphy with contrasts in rock strength. *Earth Surface Processes and Landforms*, 41(12), 1736–1757. <http://doi.org/10.1002/esp.3947>
- Gallart, F., Marignani, M., Pérez-Gallego, N., Santi, E., & MacCherini, S. (2013). Thirty years of studies on badlands, from physical to vegetational approaches. A succinct review. *Catena*, 106, 4–11. <http://doi.org/10.1016/j.catena.2012.02.008>
- Garcia-Castellanos, D., & Villaseñor, A. (2011). Messinian salinity crisis regulated by competing tectonics and erosion at the Gibraltar arc. *Nature*, 480, 359. Retrieved from <http://dx.doi.org/10.1038/nature10651>
- Gessner, K., Piazzolo, S., Güngör, T., Ring, U., Kröner, A., & Passchier, C. W. (2001). Tectonic significance of deformation patterns in granitoid rocks of the Menderes nappes, anatolide belt, Southwest Turkey. *International Journal of Earth Sciences*, 89(4), 766–780. <http://doi.org/10.1007/s005310000106>
- Gibbs, M. T., & Kump, L. R. (1994). Global chemical erosion during the Last Glacial Maximum and the present: Sensitivity to changes in lithology and hydrology. *Paleoceanography*, 9(4), 529–543.

<http://doi.org/10.1029/94PA01009>

- Haviv, I., Enzel, Y., Whipple, K. X., Zilberman, E., Matmon, A., Stone, J., & Fifield, K. L. (2010). Evolution of vertical knickpoints (waterfalls) with resistant caprock: Insights from numerical modeling. *Journal of Geophysical Research: Earth Surface*, 115(3), 1–22. <http://doi.org/10.1029/2008JF001187>
- Heineke, C., Niedermann, S., Hetzel, R., & Akal, C. (2016). Surface exposure dating of Holocene basalt flows and cinder cones in the Kula volcanic field (Western Turkey) using cosmogenic³He and¹⁰Be. *Quaternary Geochronology*. <http://doi.org/10.1016/j.quageo.2016.04.004>
- Hicks, D. M., Hill, J., & Shankar, U. (1996). Variation of suspended sediment yields around New Zealand: the relative importance of rainfall and geology. In *Erosion and Sediment Yield: Global and Regional Perspectives (Proceedings of the Exeter Symposium, July 1996)*. (pp. 149–156).
- Jetten, V., Govers, G., & Hessel, R. (2003). Erosion models: Quality of spatial predictions. *Hydrological Processes*, 17(5), 887–900. <http://doi.org/10.1002/hyp.1168>
- Kappelman, J., Alçiçek, M. C., Kazancı, N., Schultz, M., Özkul, M., & Şen, Ş. (2008). Brief communication: First Homo erectus from Turkey and implications for migrations into temperate Eurasia. *American Journal of Physical Anthropology*. <http://doi.org/10.1002/ajpa.20739>
- Kucuksezgin, F., Uluturhan, E., & Batki, H. (2008). Distribution of heavy metals in water, particulate matter and sediments of Gediz River (Eastern Aegean). *Environmental Monitoring and Assessment*, 141(1–3), 213–225. <http://doi.org/10.1007/s10661-007-9889-6>
- Lavee, H., Imeson, A. C., & Sarah, P. (1998). The impact of climate change on geo-morphology and desertification along a mediterranean arid transect. *Land Degradation and Development*, 9(SEPTEMBER), 407–422. [http://doi.org/10.1002/\(SICI\)1099-145X\(199809/10\)9:5<407::AID-LDR302>3.0.CO;2-6](http://doi.org/10.1002/(SICI)1099-145X(199809/10)9:5<407::AID-LDR302>3.0.CO;2-6)
- Lebatard, A. E., Alçiçek, M. C., Rochette, P., Khatib, S., Vialet, A., Boulbes, N., ... de Lumley, H. (2014). Dating the Homo erectus bearing travertine from Kocabaş (Denizli, Turkey) at at least 1.1 Ma. *Earth and Planetary Science Letters*. <http://doi.org/10.1016/j.epsl.2013.12.031>
- Maddy, D., Demir, T., Bridgland, D. R., Veldkamp, A., Stemerding, C., van der Schriek, T., & Schreve, D. (2007). The Pliocene initiation and Early Pleistocene volcanic disruption of the palaeo-Gediz fluvial system, Western Turkey. *Quaternary Science Reviews*. <http://doi.org/10.1016/j.quascirev.2006.01.037>
- Maddy, D., Demir, T., Bridgland, D. R., Veldkamp, A., Stemerding, C., van der Schriek, T., & Westaway, R. (2008). The Early Pleistocene development of the Gediz River, Western Turkey: An uplift-driven, climate-controlled system? *Quaternary International*. <http://doi.org/10.1016/j.quaint.2007.08.045>
- Maddy, D., Schreve, D., Demir, T., Veldkamp, A., Wijbrans, J. R., van Gorp, W., ... van der Schriek, T. (2015). The earliest securely-dated hominin artefact in Anatolia? *Quaternary Science Reviews*. <http://doi.org/10.1016/j.quascirev.2014.11.021>
- Maddy, D., Veldkamp, A., Demir, T., van Gorp, W., Wijbrans, J. R., van Hinsbergen, D. J. J., ... Aytaç, A. S. (2017). The Gediz River fluvial archive: A benchmark for Quaternary research in Western Anatolia. *Quaternary Science Reviews*. <http://doi.org/10.1016/j.quascirev.2016.07.031>

- Maddy, D., Veldkamp, A., Jongmans, A. G., Candy, I., Demir, T., Schoorl, J. M., ... van Gorp, W. (2012). Volcanic disruption and drainage diversion of the palaeo-Hudut River, a tributary of the Early Pleistocene Gediz River, Western Turkey. *Geomorphology*.
<http://doi.org/10.1016/j.geomorph.2011.12.032>
- Martínez-Casasnovas, J. A. (2003). A spatial information technology approach for the mapping and quantification of gully erosion. *Catena*, 50(2–4), 293–308. [http://doi.org/10.1016/S0341-8162\(02\)00134-0](http://doi.org/10.1016/S0341-8162(02)00134-0)
- Miall, A. D. (2015). *Stratigraphy: A modern synthesis*. *Stratigraphy: A Modern Synthesis*.
<http://doi.org/10.1007/978-3-319-24304-7>
- Mitchener, H., & Torfs, H. (1996). Erosion of mud/sand mixtures. *Coastal Engineering*, 29(1–2), 1–25.
[http://doi.org/10.1016/S0378-3839\(96\)00002-6](http://doi.org/10.1016/S0378-3839(96)00002-6)
- Riebe, C. S. (2001). Minimal climatic control on erosion rates in the Sierra Nevada, California. *Geology*, 29(5), 447–450. [http://doi.org/10.1130/0091-7613\(2001\)029<0447:MCCOER>2.0.CO;2](http://doi.org/10.1130/0091-7613(2001)029<0447:MCCOER>2.0.CO;2)
- Schoorl, J. M., Sonneveld, M. P. W., & Veldkamp, A. (2000). Three-dimensional landscape process modelling: The effect of DEM resolution. *Earth Surface Processes and Landforms*.
[http://doi.org/10.1002/1096-9837\(200008\)25:9<1025::AID-ESP116>3.0.CO;2-Z](http://doi.org/10.1002/1096-9837(200008)25:9<1025::AID-ESP116>3.0.CO;2-Z)
- Schoorl, J. M., Temme, A. J. A. M., & Veldkamp, T. (2014). Modelling centennial sediment waves in an eroding landscape - catchment complexity. *Earth Surface Processes and Landforms*, 39(11), 1526–1537. <http://doi.org/10.1002/esp.3605>
- Schoorl, J. M., Veldkamp, a, & Bouma, J. (2002). Modeling Water and Soil Redistribution in a Dynamic Landscape Context. *Soil Sci Soc Am J*, 66(5), 1610–1619. <http://doi.org/10.2136/sssaj2002.1610>
- Seyitoğlu, G. (1997). Late Cenozoic tectono-sedimentary development of the Selendi and Uşak-Güre basins: a contribution to the discussion on the development of east–west and north trending basins in western Turkey. *Geological Magazine*, 134(2), 163–175. <http://doi.org/DOI: undefined>
- Seyitoğlu, G., & Scott, B. C. (1996). Age of the Alaşehir graben (west Turkey) and its tectonic implications. *Geological Journal*, 31(1), 1–11. [http://doi.org/10.1002/\(SICI\)1099-1034\(199603\)31:1<1::AID-GJ688>3.0.CO;2-S](http://doi.org/10.1002/(SICI)1099-1034(199603)31:1<1::AID-GJ688>3.0.CO;2-S)
- Sklar, L. S., & Dietrich, W. E. (2001). Sediment and rock strength control on river incision into bedrock. *Geology*, 29(12), 1087–1090. [http://doi.org/10.1130/0091-7613\(2001\)029<1087:SARSCO>2.0.CO](http://doi.org/10.1130/0091-7613(2001)029<1087:SARSCO>2.0.CO)
- Tokçaer, M., Agostini, S., & Savaşçin, M. Y. (2005). Geotectonic setting and origin of the youngest Kula volcanics (western Anatolia), with a new emplacement model. *Turkish Journal of Earth Sciences*.
- Tucker, G. E., & Hancock, G. R. (2010). Modelling landscape evolution. *Earth Surface Processes and Landforms*, 35(1), 28–50. <http://doi.org/10.1002/esp.1952>
- van Gorp, W., Schoorl, J. M., Temme, A. J. A. M., Reimann, T., Wijbrans, J. R., Maddy, D., ... Veldkamp, T. (2016). Catchment response to lava damming: integrating field observation, geochronology and landscape evolution modelling. *Earth Surface Processes and Landforms*.
<http://doi.org/10.1002/esp.3981>
- van Gorp, W., Temme, A. J. A. M., Baartman, J. E. M., & Schoorl, J. M. (2014). Landscape evolution

- modelling of naturally dammed rivers. *Earth Surface Processes and Landforms*.
<http://doi.org/10.1002/esp.3547>
- van Gorp, W., Temme, A. J. A. M., Veldkamp, A., & Schoorl, J. M. (2015). Modelling long-term (300ka) upland catchment response to multiple lava damming events. *Earth Surface Processes and Landforms*. <http://doi.org/10.1002/esp.3689>
- van Gorp, W., Veldkamp, A., Temme, A. J. A. M., Maddy, D., Demir, T., van der Schriek, T., ... Schoorl, J. M. (2013). Fluvial response to Holocene volcanic damming and breaching in the Gediz and Geren rivers, western Turkey. *Geomorphology*. <http://doi.org/10.1016/j.geomorph.2013.07.016>
- van Hinsbergen, D. J. J. (2010). A key extensional metamorphic complex reviewed and restored: The Menderes Massif of western Turkey. *Earth-Science Reviews*, 102(1–2), 60–76.
<http://doi.org/10.1016/j.earscirev.2010.05.005>
- Van Rompaey, A. J. J., Govers, G., & Puttemans, C. (2002). Modelling land use changes and their impact on soil erosion and sediment supply to rivers. *Earth Surface Processes and Landforms*, 27(5), 481–494. <http://doi.org/10.1002/esp.335>
- Veldkamp, A., Candy, I., Jongmans, A. G., Maddy, D., Demir, T., Schoorl, J. M., ... van der Schriek, T. (2015). Reconstructing Early Pleistocene (1.3Ma) terrestrial environmental change in western Anatolia: Did it drive fluvial terrace formation? *Palaeogeography, Palaeoclimatology, Palaeoecology*. <http://doi.org/10.1016/j.palaeo.2014.10.022>
- Westaway, R., Pringle, M., Yurtmen, S., Demir, T., Bridgland, D., Rowbotham, G., & Maddy, D. (2004). Pliocene and Quaternary regional uplift in western Turkey: The Gediz River terrace staircase and the volcanism at Kula. *Tectonophysics*. <http://doi.org/10.1016/j.tecto.2004.07.013>
- Yair, A., & Lavee, H. (1980). Runoff and Erosion Processes and Rates in the Zin valley badlands, northern Negev, Israel. *Earth Surface Processes*, 225, 205–225.